SENCKENBERG

CrossMark

Calcinea of the Red Sea: providing a DNA barcode inventory with description of four new species

Oliver Voigt[1] · Dirk Erpenbeck[1,2] · Rául A. González-Pech[1] · Ali M. Al-Aidaroos[3] ·
Michael L. Berumen[4] · Gert Wörheide[1,2,5]

Abstract The Red Sea is a biodiversity hotspot with a considerable percentage of endemic species for many marine animals. Little is known about the diversity and distribution of calcareous sponges (Porifera, Class Calcarea) in this marginal sea. Here we analysed calcareous sponges of the subclass Calcinea that were collected between 2009 and 2013 at 20 localities in the Red Sea, ranging from the Gulf of Aqaba in the north to the Farasan Islands in the south, to document the species of this region. For this, we applied an integrative approach: We defined OTUs based on the analyses of a recently suggested standard DNA marker, the LSU C-region. The analysis was complemented with a second marker, the internal transcribed spacer, for selected specimens. Ten OTUs were identified. Specimens of each OTU were morphologically examined with spicule preparations and histological sections. Accordingly, our ten OTUs represent ten species, which cover taxonomically a broad range of the subclass. By combining molecular and morphological data, we describe four new species from the Red Sea: *Soleneiscus hamatus* sp. nov., *Ernstia arabica* sp. nov., *Clathrina rotundata* sp. nov., and *Clathrina rowi* sp. nov.. One additional small specimen was closely related to "*Clathrina*" *adusta*, but due to the small size it could not be properly analysed morphologically. By providing the DNA sequences for the morphologically documented specimens in the Sponge Barcoding Database (www.spongebarcoding.org) we facilitate future DNA-assisted species identification of Red Sea Calcinea, even for small or incomplete samples, which would be insufficient for morphological identification. Application of DNA barcode methods in the subclass will help to further investigate the distribution of Calcinea in the Red Sea and adjacent regions.

Keywords Porifera · Calcarea · Red Sea · DNA barcoding · Taxonomy

✉ Oliver Voigt
oliver.voigt@lmu.de

1 Department of Earth and Environmental Sciences, Palaeontology and Geobiology, Ludwig-Maximilians-Universität München, Richard-Wagner-Str. 10, 80333 Munich, Germany

2 GeoBio-Center, Ludwig-Maximilians-Universität München, Richard-Wagner-Str. 10, 80333 Munich, Germany

3 Faculty of Marine Sciences, Marine Biology Department, King Abdulaziz University, P.O. Box 80207, Jeddah 21589, Kingdom of Saudi Arabia

4 Red Sea Research Center, King Abdullah University of Science and Technology, 23955-6900 Thuwal, Kingdom of Saudi Arabia

5 Bayerische Staatssammlung für Paläontologie und Geologie, Richard-Wagner-Str. 10, 80333 Munich, Germany

Introduction

The Red Sea is a marine biodiversity hotspot with many endemic animal species (DiBattista et al. 2016). Knowledge about the diversity and distribution of sponge species in the Red Sea is scarce with few exceptions (Keller 1889, 1891; Row 1909; Erpenbeck et al. 2016). In particular, the often small, inconspicuous species of calcareous sponges (Porifera, class Calcarea) are understudied in the Red Sea. Most reports on calcareous sponge species from the Red Sea are based on material collected

over 100 years ago. The recognized species from the region were described by Haeckel (1872), Row (1909) and Klautau and Valentine (2003). The most comprehensive study on calcareous sponges of the Red Sea was the study on the Crossland collection by Row (1909), who reported six calcinean species. However, all but one of the species in this work were only represented by one or two specimens (Row 1909):

1) *Clathrina sinusarabica* Klautau and Valentine, 2003, original identification: *Clathrina coriacea* (Montagu, 1818), 2 specimens
2) *Clathrina primordialis* (Haeckel, 1872), 1 specimen
3) *Arthuria sueziana* (Klautau and Valentine, 2003), original name *Clathrina canariensis* var. *compacta* Row, 1909, 1 specimen
4) *Arthuria tenuipilosa* (Dendy, 1905), original name *Clathrina tenuipilosa* Dendy, 1905, several specimens (number undefined)
5) *Leucetta primigenia* Haeckel 1872, mentioned as *Leucandra primigenia*, 1 specimen
6) *Leucetta microraphis* Haeckel, 1872, mentioned as *Leucandra primigenia* var. *microraphis,* 2 specimens.

Increased specimen and taxon sampling is required to understand the diversity and distribution of calcinean species in the Red Sea. In recent years molecular studies revealed that most classical recognized taxa of calcareous sponges based on morphological characters are in strong conflict with molecular phylogenies (Manuel et al. 2003; Dohrmann et al. 2006; Voigt et al. 2012a). These observations were attributed to a high level of morphological homoplasy (Manuel et al. 2003). Consequently, a new species description based only on morphological characters potentially provides little information about phylogenetic affinities. It was suggested that comprehensive systematic and taxonomic studies of this sponge group should no longer be based solely on morphological characters, but on combined analysis of DNA and morphological data in integrative approaches (Rossi et al. 2011; Voigt et al. 2012a; Voigt and Wörheide 2016). Such studies became important tools in calcareous sponge taxonomy (e.g., Imešek et al. 2014; Azevedo et al. 2015; Klautau et al. 2016) and since have guided substantial reorganization and introduction of new genera in the subclass Calcinea (Klautau et al. 2013). We recently proposed to use a short variable fragment of the large subunit ribosomal RNA (LSU or 28S rRNA gene), the C-region, as a standard marker for integrative approaches for studies of Calcarea, which potentially is also a good marker for DNA-based species determination in this sponge class (Voigt and Wörheide 2016). An alternative, more variable marker that has been used in taxonomic approaches is the internal transcribed spacer region (ITS, including ITS1, 5.8S, and ITS2), which, however, has also certain difficulties such as intragenomic length polymorphisms (Wörheide et al.

2004). ITS sequences are also difficult to align due to the high amount of indels. Therefore it is problematic to include suitable outgroup sequences, and consequently most calcinean ITS phylogenies are arbitrarily or mid-point rooted (as discussed in Voigt and Wörheide 2016). We here applied an integrative taxonomic approach to study the diversity of Calcinea of the Red Sea from specimens collected between 2009 and 2013, with the aim to provide a comprehensive DNA barcode database for this region. For this, we combined DNA analysis with morphological observations. Our DNA analysis focuses on the C-region of the LSU, for which data of more genera was available. Because for some additional species only ITS data exists, this marker was also applied.

Material and methods

Sample collection and sample documentation

Forty-six specimens of Calcinea were collected at 20 localities between 2009 and 2013 by scuba diving or snorkelling in the Red Sea from the Gulf of Aqaba in the north to the Farasan Islands in the south (Fig. 1, Suppl. Table 1). If possible, photos were taken *in situ* before sampling and after sampling before fixation. Sponges were fixed and stored in 70–90% ethanol. Most specimens were documented by photography using a Leica M165FC stereomicroscope before further manipulation. To increase focal depth of the photos, stacks of images were taken and later combined in a focussed image using Helicon Focus 4.2.9 (HeliconSoft). Small pieces of tissue were cut from each specimen with a scalpel blade for subsequent DNA isolation. Additional pieces were cut from selected specimens to prepare spicule preparations and microscopic sections. Spicules were cleaned from soft tissue by incubating the cut sponge piece for several hours in a household-grade bleach solution (containing 4% sodium hypochlorite). After the tissue was dissolved, the spicules were cleaned five times with distilled water, transferred to microscope slides, dried and mounted with Eukitt (Sigma-Aldrich). For selected species, spicules were observed by scanning electron microscopy (SEM). For this, the spicules were mounted on SEM stubs, sputter-coated with gold, and imaged using a Hitachi SU5000 SEM.

For sections, sponge tissue was dehydrated with increasing ethanol concentrations (30%, 50%, 70%, 100%), stained overnight in an acidic Fuchsine solution in ethanol, and embedded in LR White Resin (Plano) as described before (Voigt et al. 2012a). Sections of 10–200 μm thickness were cut from the resin block with a Leica 1600 saw microtome and mounted to microscope slides with Eukitt (Sigma-Aldrich). Some sections were stained on the surface with a Fuchsine-Toluidine solution to visualize the cells on the section's surface before mounting (Voigt et al. 2012a). Spicule preparations and sections were
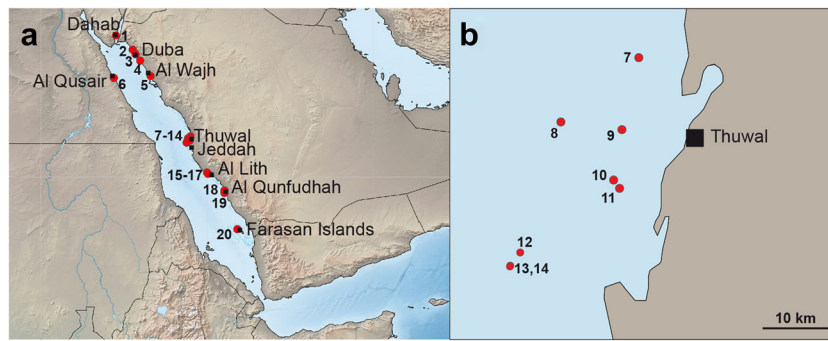
Fig. 1 Sample localities of calcinean specimens. **a** Overview. **b**: Details of the Thuwal region. Red dots depict sample localities; black squares depict the close named towns/regions. **1**: Egypt, Dahab; **2–4**: Saudi Arabia, near Duba; **5**: Saudi Arabia, Al-Wajh; **6**: Egypt, S of Al Qusair; **7–14**: Reefs near Thuwal (7: Quita al Kirsh W, 8: Shi'b Nazar S; 9: Palace Reef N; 10: Shi'b Esfenj; 11: Sodfa; 12: Abu Madafi N; 13: Abu Madafi channel; 14: Abu Madafi centre); **15–17**: Saudi Arabia, NE of Al Lith (three localities); **18**: Saudi Arabia, N of Qunfudhah; **19**: Saudi Arabia, Reef near Qunfudhah, **20**: Saudi Arabia, Farasan Islands. See also Suppl. Table 1 for GPS coordinates

documented with a Leica DFC480 camera on a Leica DMLB compound microscope. Measurements of spicules were performed in imageJ (Abràmoff et al. 2004) after scale calibration. Actine length was measured from tip to base, actine width was measured at the actine base in triactines and tetractines, and at the widest part in diactines (and trichoxeas). Three actines per spicule were measured for triactines and the basal system of tetractines. Spicule measurements are provided as minimum – <u>mean</u> (standard deviation, SD) – maximum. Specimens were deposited in the collections of the King Abdulaziz Marine Museum, King Abdulaziz University, Jeddah, Saudi Arabia (KAUMM), the Senckenberg Museum Frankfurt, Germany (SMF), and the Paleontological State Collection, Munich, Germany (SNSB-BSPG). Additional voucher subsamples of some specimens are kept at the King Abdullah University of Science and Technology, Jeddah, Saudi Arabia in the collections of the Berumen lab. Maps of sample localities were generated with SimpleMappr (http://www.simplemappr.net, Shorthouse 2010).

DNA extraction, PCR and sequencing

DNA was isolated with a previously described method using a 96-well AcroPrep1 µm glass fiber plate (PALL Life Sciences) and guanidinium thiocyanate solution for DNA-binding (Vargas et al. 2012). 1 ng of DNA was added as template in PCR reactions (total volume 25 µL). The C-region of the LSU was amplified by PCR (thermo-profile: 96 °C: 3 min; 35× [96 °C:30s, 52 °C:30s; 72 °C: 30s]; 72 °C:3 min) using the following primers: fwd: 5'-GAAAAGAACTTTGRARAGAGAGT-3', rv: 5'-TCCGTGTTTCAAGACGGG-3' (Chombard et al. 1998). ITS (ITS1, 5.8S, ITS2) of selected samples was amplified by PCR (thermo-profile: 96 °C: 3 min; 35× [96 °C:30s, 52 °C:30s; 72 °C: 1 min]; 72 °C:3 min) with the primers: fw: 5'- GTCCCTGCCCTTTGTACACA-3'; rv: 5'-CCTGGTTA GTTTCTTTTCCTCCGC-3' (Adlard and Lester 1995). Bi-directional DNA-sequencing of the PCR fragments was prepared

with the BigDye Terminator Sequencing Kit v.3.1 (Applied Biosystems), and performed at the Sequencing Service of the LMU Biozentrum on an ABI 3730 capillary sequencer (Applied Biosystems). Forward and reverse sequences were assembled in Geneious R8 (http://www.geneious.com, Kearse et al. 2012) or CodonCode Aligner (www.codoncode.com) and checked by eye for correct base-calling. Sequences were submitted to NCBI GenBank (accession numbers KY366357-KY366410, KY701522, KY711435, KY775298). DNA-sequences of the C-region and the ITS region of the holotypes of new species described here and of one representative of each other species are also available at the sponge barcoding website (www.spongebarcoding.org, IDs 1650-166 4) along with morphological descriptions of the specimens.

DNA alignment and definition of OTUs

Sequences of the C-region of LSU were added to an existing alignment of calcareous sponges, which included information on the region's secondary structure (Voigt and Wörheide 2016) in SeaView (Gouy et al. 2010). The full alignment with information of the selected sites is available at the Sponge Gene Tree Server (www.spongenetrees.org). The complete C-region was used to compare pairwise distance between samples. Potential OTUs were determined by an initial neighbor-joining tree calculated in Seaview and defined as samples forming a monophyletic clade >99% sequence similarity and with sisterclades of Calcinea from different regions than the Red Sea. After pairwise distance calculation, thorough phylogenetic analyses were performed (see below). Each OTU represented a different species, which was further morphologically analysed. We inspected the overall morphology from the specimen photographs and documented the spicules and/or the sections as described above. These observations were compared to species descriptions of calcareous sponge species reported from the Red Sea (Haeckel 1872; Row 1909; Klautau and Valentine 2003) or of potentially related species. In some

cases, ITS data was available for additional taxa, which potentially were closely related to the defined OTUs. Therefore, ITS sequences from Calcinea were analysed, too. However, the ITS alignment contained about 50% gaps due to the high level of variability that did not allow an unambiguous alignment of all sites over all taxa. Therefore, we excluded sites of uncertain homology under the guidance of Gblocks (Castresana 2000) as implemented in Seaview. The resulting dataset contained 499 positions. This reduction of the dataset decreases phylogenetic noise (between distantly related species) at the cost of lower resolution between closer related species.

Phylogenetic analyses

From the LSU dataset (511 bp) we excluded sites outside of the C-region and sites of uncertain homology from the phylogenetic analyses, resulting in a dataset of 394 positions. The ITS alignment contained 1617 bp, the average sequence length in the alignment was 813 bp. After exclusion of ambiguously aligned sites, the ITS dataset comprised 499 positions. For further phylogenetic analyses of the LSU, identical sequences were collapsed into single sequences using DNAcollapser in FaBox (Villesen 2007). Jmodeltest 2.7.1 (Posada 2008) was used to find the best standard nucleotide evolutionary model for the datasets (C-region LSU: TPM2uf + I + G; ITS: SYM + I + G). We used PhyML 3.0 (Guindon et al. 2010) to run a Maximum Likelihood (ML) analysis with 200 bootstrap replicates. For LSU, a Bayesian analysis was performed in PHASE 3 with RNA-specific substitution models (Telford et al. 2005). To determine a suitable combination of standard model for loop and RNA model for paired sites in PHASE 3 we used the script "model-selection.pl" (Allen and Whelan 2014), for which we provided the best ML tree under the best standard nucleotide model as input tree. The model-testing using AIC suggested the model combination REV (=GTR) + G for unpaired and RNA16A + G for paired sites as optimal RNA model combination. Four independent Bayesian analyses were performed in PHASE 3 with the *mcmcphase*-command, each was run for 10 million generations, of which every 200th tree was sampled after a burnin-phase of one million generations. Trees were summarized with the *mcmcsummarize* command. We used Tracer v 1.6 (http://tree. bio.ed.ac.uk/software/tracer/) to monitor the parameter sampling of each run. Readable input files for Tracer were generated with a modified Perl script phase2tracer.pl from Matt Yoder (http://hymenoptera.tamu.edu/rna/download.php). For ITS, Bayesian inference was conducted with MrBayes (Ronquist and Huelsenbeck 2003). Two runs with four chains were run for 10 million generations, of which every 200th tree was sampled. The consensus tree was calculated with the *sumt*-command and with the first 25% of sampled trees omitted as burnin. The posterior probability support of the Bayesian inferences were added to the ML tree topologies. Datasets and trees obtained by our analysis and the datasets are available on the

Sponge Genetree Server (www.spongegenetrees.org, Erpenbeck et al. 2008).

Results

Phylogenetic analyses and identification of OTUs

With our phylogenetic analyses of the C-region of the LSU we identified 10 OTUs. These were monophyletic clades containing one to 11 specimens with 99.5 to 100% sequence identity (Fig. 2). The taxonomic diversity of the OTUs was high as they are widely distributed over the calcinean tree (Fig. 2).

The reconstructed LSU phylogeny is similar to trees of previous studies with the same marker (Voigt and Wörheide 2016), and largely congruent with the ITS phylogenies (Suppl. Fig. 1). The position of the root of Calcinea and several basal nodes did not find high bootstrap (BS) support, but the posterior probability (PP) is sometimes high for these nodes. The first branching species of the genera *Ascandra* and *Soleneiscus* were not monophyletic, and *Levinella* did fall in one clade with two *Ascandra* species. The genera *Ernstia*, *Brattegardia*, *Borojevia,* and *Leucettusa* found high support, while *Clathrina* sensu Klautau et al. 2013 and a clade of *Leucetta* and *Pericharax* (=Leucettidae) were recovered in both analysis, but with lower BS support (Fig. 2). The tetractine-bearing "*Clathrina*" *adusta* together with two undetermined "*Clathrina*" (*sensu lato*) specimens were a sisterclade to the *Clathrina* sensu Klautau et al. 2013, which lack tetractines. The sister group relationship of these found high BS and PP support. The relationships of *Arthuria sueziana*, *Ascaltis reticulum*, *Murrayona phanolepis, Lellapiella incrustans*, and *Leucaltis nodusgordii* was not highly supported and differed in the Bayesian analysis. Similarly, the sistergroup relationship of *Borojevia* and *Brattegardia* was only found in ML (and here with low support). *Leucettusa* formed a sisterclade to Leucettidae, with low BS and high PP support.

In the LSU tree, the Calcinean specimens fell into 10 clades that fit our OTU definition. We recovered a sistergroup relationship of OTU 1 (*Soleneiscus hamatus* sp. nov.) to *Soleneiscus radovani* (BS: 77%; PP: 63%). OTU 2 formed a clade with *Ernstia tetractinia* and two undetermined species of *Ernstia*. OTU 3 was very closely related to "*Clathrina*" *adusta* (BS & PP: 100%). The specimen like *Clathrina adusta* possesses tetractines (see below). Three OTUs (OTU 4–6) were found within *Clathrina* sensu Klautau 2013. OTU 4 (*Clathrina rotundata* sp. nov.) was the sister taxon to the clade of *Clathrina ramosa* and *Clathrina blanca* (BS & PP: 100%). The analysis of ITS also indicated a close relationship to *Clathrina hispanica* (Suppl. Fig. 1). OTU 5 (*Clathrina sinusarabica*) and OTU 6 (*Clathrina rowi* sp. nov.) were found in one clade with *Clathrina luteoculcitella* (BS: 89%; PP: 99%), in which the latter two were a sisterclade to OTU 5 (BS:<50, PP:92). The position of OTU 7 (*Arthuria sueziana*)
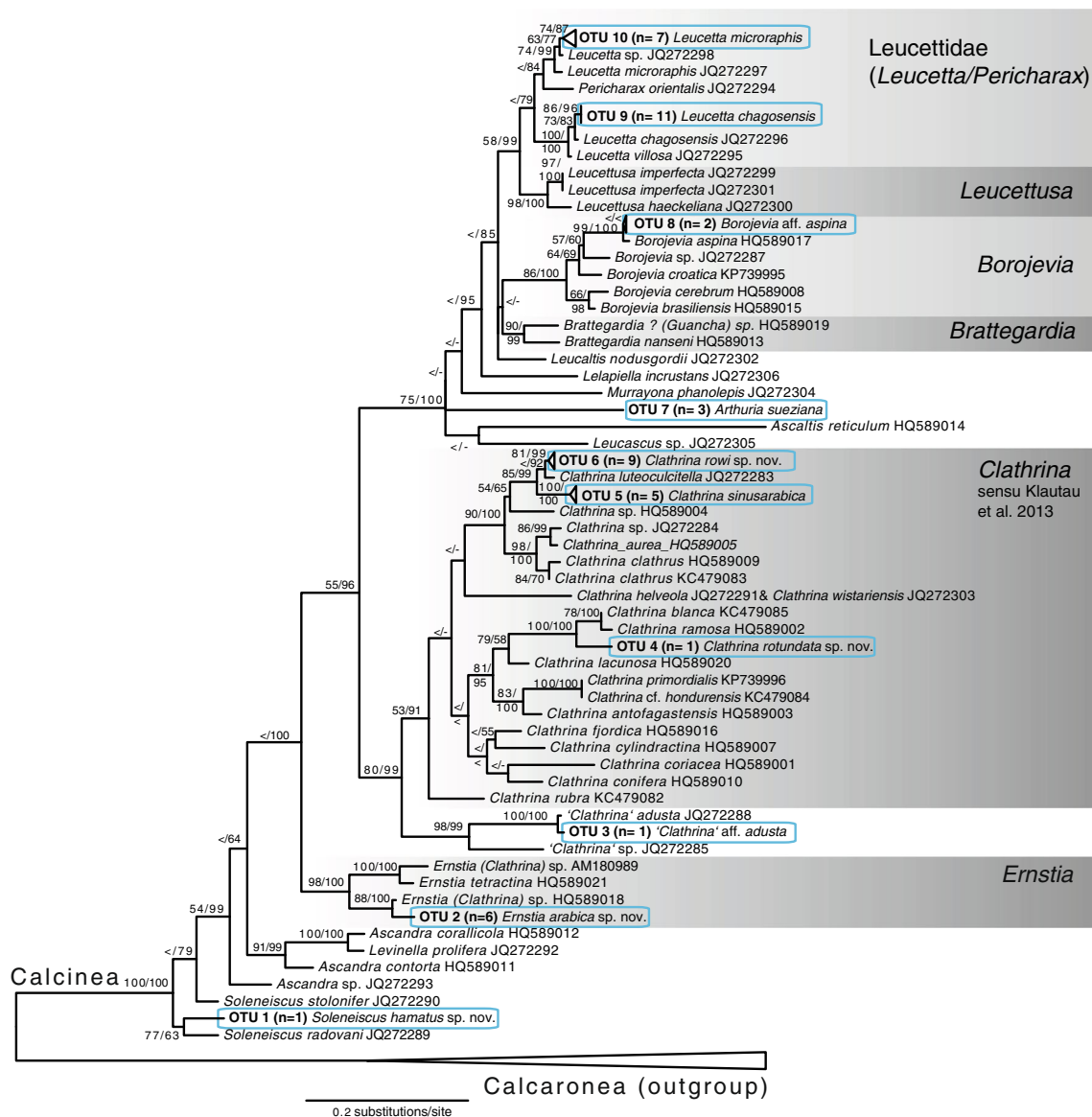
Fig. 2 ML phylogeny of the C-region of LSU dataset. Calcaronea (36 species) were used as outgroup (Suppl. Table 1). Positions of OTUs are highlighted, their clades are shown collapsed. Support values are shown at the nodes (Bootstrap/Posterior Probability in percent, < = values below 50, - = node not present in Bayesian phylogeny)

did not find support in the LSU dataset (other specimens of the genus are not available), but the ITS phylogeny revealed that it formed a clade with *Arthuria hirsuta* (BS: 99%; PP: 100%, Suppl. Fig. 1). *Borojevia aspina* and OTU 8 (*Borojevia* aff. *aspina*) were sistertaxa in the LSU analyses (BS: 99%; PP: 100%). In the ITS trees, *B.* aff. *aspina* is nested within *B. aspina* in the ML tree (low BS of 50), but not the Bayesian phylogeny (Suppl. Fig. 1). OTU 9 (*Leucetta chagosensis*) was closest related to another *Leucetta chagosensis* specimen (BS: 73%; PP: 88%, Fig. 2). OTU 10 (*Leucetta microraphis* was closest related to an undetermined *Leucetta* species, with which it formed a sisterclade to *Leucetta microraphis* (for the latter clade: BS: 74%; PP: 99%, Fig. 2).

Undetermined specimen: "*Clathrina*" aff. *adusta* (OTU 3)

(Figure 3a-c).

The specimen (SMF11618) is very small (2 mm × 1 mm) and was growing on another sponge sample. Our DNA analysis (Fig. 2) places it in close relationship to "*Clathrina*" *adusta*. The cormus is formed by few anastomosing tubes (Fig. 3a) and the skeleton contains triactines and tetractines with (in case of tetractines basal) actines about 66–73 µm × 9–10 µm (Fig. 3b). Beaause of its small size it was not possible to provide a detailed morphological description here. Since it is the only specimen of OTU 3 in our collection and genetically distinct from the other reported species, its occurrence is
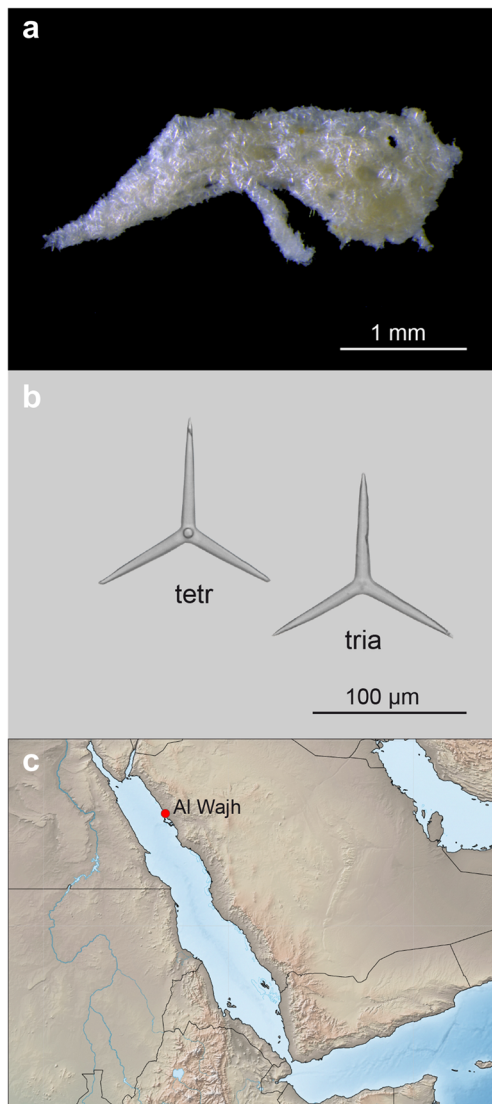
Fig. 3 *Clathrina* aff. *adusta* (OTU 3). **a** SMF11618, fixed specimen. **b** Spicules: Triactines and tetractines. **c** Locality of collected specimen. tetractine, tria = triactine

worth mentioning. It was collected near Al-Wajh (Saudi Arabia, N26.058278° E36.594725°, Fig. 3c).

Description of species

Phylum Porifera Grant, 1836
    Class Calcarea Bowerbank, 1864
    Subclass Calcinea Bidder, 1898
    Order Clathrinida Hartman, 1958
    Family Dendyidae De Laubenfels, 1936
    Diagnosis

"Clathrinida with an essentially tubular organisation, forming an individual ascon tube (olynthus) with several tubes growing from the basal stolon-like tubes or forming distally ramified, but not anastomosed tubes radially arranged around a central olynthus without any special skeletal differentiation.

A continuous choanoderm lines all the internal cavities. Spicules are regular triactines and/or tetractines, to which tripods or diactines may be added." (Borojević et al. 1990).

Remarks

The family Soleneiscidae (Borojević et al. 1990) represents a junior synonym to Dendyidae (Azevedo et al. 2015). The diagnosis of the genus is the more detailed one that was provided by Borojević et al. (1990), as suggested previously (Azevedo et al. 2015).

Genus *Soleneiscus* Borojević, Boury-Esnault, and Vacelet, 1990

Diagnosis

Dendyidae "that grow in form of an individual ascon tube, with several ascon tubes growing upright from basal stolon-like tubes, or in the form of creeping, distally-ramified but only rarely anastomosing tubes." (Borojević et al. 2002).

Soleneiscus hamatus sp. nov. Voigt, Erpenbeck, and Wörheide

(Figure 4a-h).

Diagnosis: *Soleneiscus* with yellow tubes (in life), which are connected at their base. The skeleton contains two types of tetractines (type I and II): tetractines type I have apical actines that are on average wider than the basal actines; tetractines type II have apical actines which are less than half of the width of the basal actines and are frequently bent near their tips in a ca. 45–90° angle, giving them a hook-like appearance. Perpendicular diactines are present.

Type Material: Holotype SNSB-BSPG GW2975.

Etymology: Latin *hamatus* (=hooked). Named for the hook-like appearance of the apical actines of one type of tetractines (tetractines II) of the species.

Material examined: SNSB-BSPG GW2975 (1 specimen).

Type locality: S of Al Qusair, Egypt, N25.943031° E34.389128°, 5–10 m depth, coll. G. Haszprunar.

Colour: Yellow in life, white in 80% ethanol.

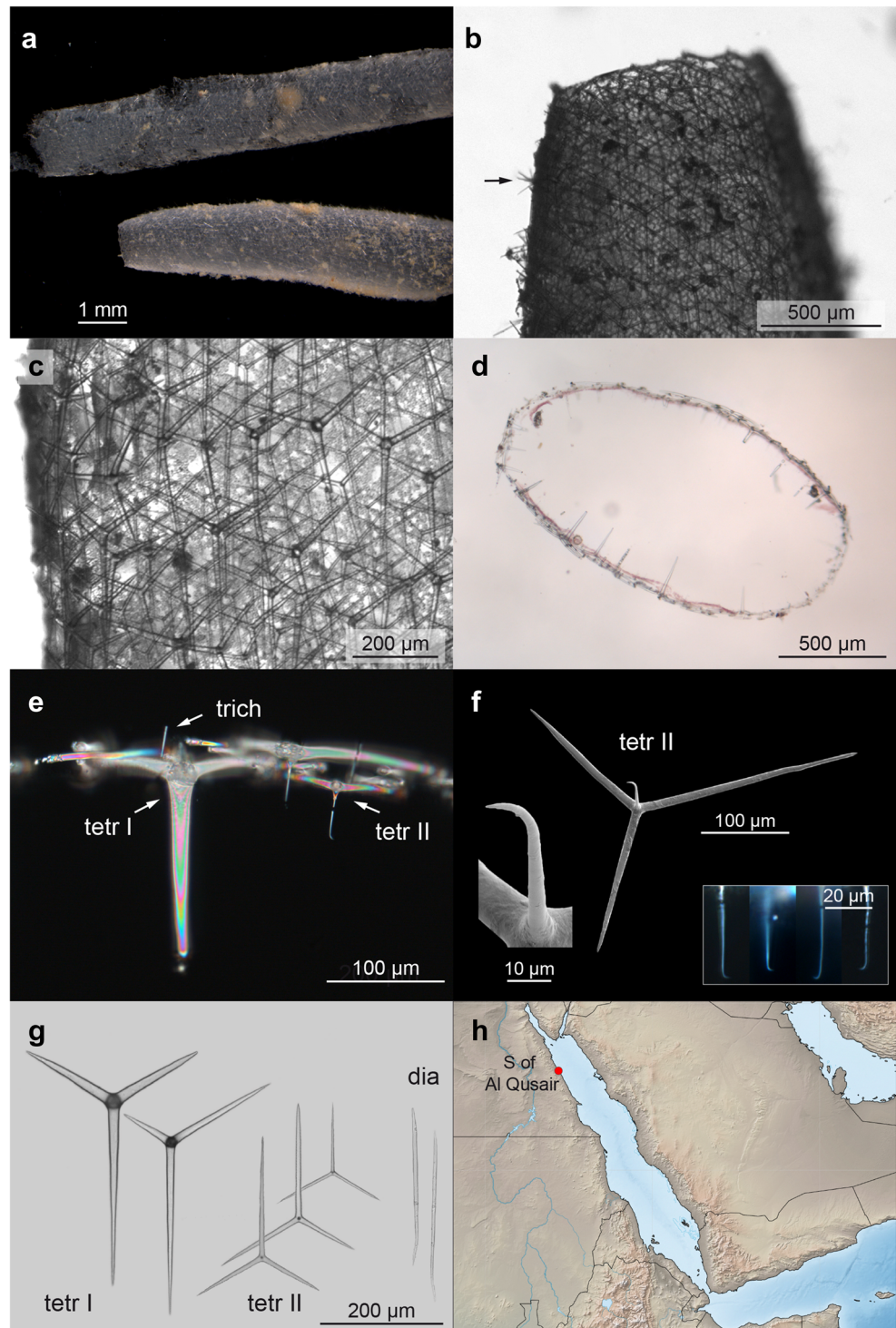**OTU (C-region):** OTU 1 ($n = 1$).

Growth form: Single tubes, about 1.3 mm in diameter, with an apical osculum, originally only united at their base, now separated (Fig. 4a, b).

Aquiferous system: Asconoid, the choanoderm is not folded (Fig. 4d).

Skeleton: Tetractines of two types (tetractines I with thick apical actines, tetractines II with thin apical actines), their basal actines supporting the tube wall, the apical actines reaching into the atrium (Fig. 4c-f). Occasional diactines, perpendicular to the sponge wall, are protruding to the outer side (Fig. 4b). Some smaller perpendicular trichoxea-like diactines can be observed in the sponge wall, but are broken off in the sections and were not detected in the spicule preparations.

Spicules: Two types of tetractines (tetractines I with thick apical actines, tetractines II with thin apical actines), diactines and occasional trichoxeas (Fig. 4e-g).

Fig. 4 *Soleneiscus hamatus* sp. nov. (OTU1). **a** Fixed holotype (SNSB-BSPG GW2975). **b** Detail of the oscular region. The arrow points at perpendicular diactines protruding from the sponge wall. **c** Tetractines in the sponge wall, their unpaired actine pointing away from the osculum, **(d)** Transversal section, showing the asconoid aquiferous system and the apical actines of tetractines that protrude into the tube. **e** Apical actines of tetractine I (tetr I) and tetractines II (tetr II), and a broken trichoxea-like spicule (trich). **f** SEM image of a tetractine II with a hook-like apical actine. Inset: Light microscopy of the hook-like apical actines of tetractine II as observed in sections. **g** Spicules: Tetractines I, tetractines II and diactines (dia). **h** Type locality. dia = diactines, tetr = tetractine, tria = triactine, trich = trichoxea

Tetractines I: Basal system equiangular, parasagittal to equiradiate, sometimes all three basal actines differ in length. Basal actines are conical and have sharp tips. Apical actines are on average thicker at their base than the actines of the basal triradiate system, straight or slightly bent, sometimes hooked (Fig. 4e, g). Tetractine I dimensions are: Basal triradiate system: 84–179.5 (SD 49.1)–291 μm × 9–13.0 (SD 90.7)–19 μm (*n* = 20) [unpaired actine of parasagittal tetractines: 199–251.1 (SD 24.1)–291 μm × 9–13.5 (SD 3.1)–19 μm (*n* = 16); paired actines 84.2–156.6 (SD 32.3)–272 μm × 10–13.5 (SD 2.8)–19 μm (*n* = 16)]. Apical actines were measured in sections: 120–147.3 (SD 16.1)–167 μm × 13–18.1 (SD 4.0)–27 μm (*n* = 11).

Tetractines II: Basal system equiangular, parasagittal to equiradiate, sometimes all three actines differ in length (Fig. 4g). Basal actines are conical and have sharp tips. The apical actines are much thinner than the actines of the basal triradiate system and sometimes have a hook-like bent near their tips (Fig. 4f). Straight apical actines also occur. Tetractine II dimensions are: Basal triradiate system: 68–134.2 (SD 37.0)–235 μm × 5–8.7 (SD 2.4)–15 μm ($n = 20$) [unpaired actines of parasagittal tetractines: 115–179.6 (SD 31.9)– 235 μm × 5–9.0 (SD 2.3)–15 μm ($n = 13$); paired actines: 80–117.7 (SD 19.0)–152 μm × 5–8.9 (SD 2.4)–14 μm ($n = 13$)]. Apical actines were measured in sections: 35–41.8 (SD 3.2)–49 μm × 3–3.5 (SD 0.6)–5 μm ($n = 20$).

Diactines: Straight diactines with two pointed tips, sometimes slightly bent near the end of one tip (Fig. 4g). Diactine dimensions are: 136–207.6 (SD 42.6)–274 μm × 5–6.2 (SD 0.8)–8 μm ($n = 10$). Smaller, broken trichoxea-like diactines were only observed in sections and were of about the same diameter as the apical actines of tetractines II.

Ecology: The specimen was growing on hard substrate on the underside of an overhang without direct sunlight. A specimen of *Leucetta chagosensis* (SNSB-BSPG GW2973, see below) was found growing close by under similar conditions.

Distribution: The type locality at the coast of Egypt, south of Al Qusair (Fig. 4h), is the only record for this species.

Remarks: Currently eight species are recognized in the genus. In our LSU phylogeny, *Soleneiscus radovani* Wörheide and Hooper 1999 was most closely related to *S. hamatus* sp. nov..

Soleneiscus hamatus sp. nov. can be distinguished from most species by the combination of spicule types and categories. In contrast to *S. hamatus* sp. nov. the following species lack diactines: *Soleneiscus apicalis* (Brønsted, 1931), *Soleneiscus japonicus* (Haeckel, 1872), *Soleneiscus radovani* Wörheide and Hooper, 1999; *Soleneiscus pedicellatus* Azevedo, Cóndor-Luján, Willenz, Hajdu, Hooker, and Klautau, 2015 lacks diactines and tetractines. *Soleneiscus olynthus* (Borojević and Boury-Esnault, 1987) and *Soleneiscus hispidus* (Brønsted, 1931) do not have two categories of tetractines. More similar to the new species are *Soleneiscus stolonifer* (Dendy, 1891) and *Soleneiscus irregularis* (Jenkin, 1908). In both species, two types of

tetractines with different sizes of apical actines were reported (Table 1). However, in *S. stolonifer*, the apical actines of tetractines I can exceed the length of their basal actines by the factor three, reaching up to 600 μm (Dendy, 1891), which was not observed in *S. hamatus* sp. nov., where they are on average shorter than the basal actines (Table 1). In *S. irregularis*, tetractines I have apical actines that are as thick as its basal actines, while in *S. hamatus* sp. nov. the apical actines of tetractines I are thicker than the corresponding basal actines. The apical actines of tetractines II are longer and thicker in *S. irregularis* compared to *S. hamatus* sp. nov. (Table 1). Diactines in *S. stolonifer* and *S. irregularis* are much larger than in *S. hamatus* sp. nov. (Table 1). However, an Australian specimen (QM G313668) that had been attributed to *S. stolonifer* (Wörheide and Hooper 1999) had diactines within the range of diactines of *S. hamatus* sp. nov.. It differs in the life colour (white) and also has a divergent DNA sequence from *S. hamatus* sp. nov. (Fig. 2). However, like the type specimen of *S. stolonifer* and *S. irregularis*, it lacked the hook-like bents on the apical actines that occur *S. hamatus* sp. nov.. Additional samples of all three species will be necessary to understand their relationships.

Family Clathrinidae Minchin,1900

Diagnosis "Clathrinida with an essentially tubular organisation. The skeleton is formed by tangential triactines, to which tripods, tetractines, and diactines may be added. A continuous choanoderm lines all the internal cavities. The water crosses the wall through pores, delimited by porocytes. The young sponges have an olynthus form that grows through longitudinal median division, budding and anastomosis of individual tubes, forming large units called the 'cormus'. There is neither a common cortex nor a well-defined inhalant or exhalant aquiferous system." (Borojević et al. 2002).

Genus *Ernstia* Klautau, Azevedo, Cóndor-Luján, Rapp, Collins, and Russo, 2013

Diagnosis: "Calcinea in which the cormus comprises a typical clathroid body. A stalk may be present. The skeleton contains regular (equiangular and equiradiate) and/or sagittal triactines and tetractines. Tetractines are the most abundant spicules or occur at least in the same proportion as the

Table 1 Comparison of spicule dimensions of *S. hamatus* sp. nov., *S. irregularis*, and *S. stolonifer*

	S. hamatus nov. sp.	*S. irregularis*	*S. stolonifer*
Tetractines I (basal actines)	84–291 μm × 9–13 μm	150–220 μm × 20 μm	200 μm × 15 μm
Tetractines I (apical actines)	120–167 μm × 13–27 μm	210–260 μm × 16–20 μm	up to 600 μm
Tetractines II (basal actines)	68–235 μm × 5–15 μm	100–200 μm × 10–16 μm	200 μm × 15 μm
Tetractines II (apical actines)	35–49 μm × 3–5 μm	120–150 × 7μm	much shorter than facial rays, slender
Diactines	136–274 μm × 5–8 μm	300–800 μm × 21–24 μm	700 × 30 μm

Measurements of *S. irregularis* from Jenkin (1908), measurements of *S. stolonifer* from Dendy (1891)

triactines. Tetractines frequently have very thin (needle-like) apical actines. Diactines may be added. Asconoid aquiferous system." (Klautau et al. 2013).

Ernstia arabica sp. nov. Voigt, Erpenbeck, and Wörheide (Figure 5a-e, Table 2, Suppl. Fig. 2).

Diagnosis: *Ernstia* with yellow cushion-shaped to sub-spherical cormi of tightly anastomosed tubes with one or few water-collecting tubes. The skeleton includes tetractines and triactines, trichoxea-like diactines may be numerous or be missing. Triactines and tetractines have conical actines with blunt tips. Compared to other species, the actines of the basal triradiate system of triactines and tetractines have a smaller length to width ratio (triactines in average 7.7, basal system of tetractines in average 7.4). The apical actines of tetractines are thinner than the basal actines (average length/width ratio in the holotype: 12.4).

Type Material: Holotype SMF11627.

Paratypes: Porifera-KAUMM-7, Porifera-KAUMM-8.

Etymology: Latin *arabica* (=arabic). Named for its distribution along the coast of the Arabian Peninsula.

Material examined: 6 specimens: SMF11627, SNSB-BSPG GW1130, Porifera-KAUMM-8, SMF11578, Porifera-KAUMM-6, Porifera-KAUMM-7.

Type locality: SMF11627: Farasan Island (NW), Saudi Arabia, N16.86596° E41.80983°, 5 m depth, coll. O. Voigt, 25 February 2012.

Additional material: SNSB-BSPG GW1130: Gulf of Aqabar, Dahab, Egypt, N28.48° E34.513°, 2 m, 2 October 2009; SMF11578, Porifera-KAUMM-6: N of Duba, Saudi Arabia, N27.61866° E35.519667, 0.5 m, coll. D. Erpenbeck, 19 June 2013; Porifera-KAUMM-7, Porifera-KAUMM-8: S

of Duba, Saudi Arabia, N26.963058° E35.966444°, 0.5 m, coll. D. Erpenbeck, 20 June 2013.

OTU (C-region): OTU 2, sequence identity 100% ($n = 6$).

Colour: Yellow in life (Suppl. Fig. 2), pale brown in 70%–90% ethanol.

Growth form: Cushion-shaped to sub-spherical cormi of tightly anastomosed tubes with one to several oscula at the end of water-collecting tubes (Fig. 5a, Suppl. Fig. 2). The tubes of the holotype (Fig. 5a-c) have a diameter of 210–220 μm. The specimen was fragmented during collection. The holotype contains oocytes.

Skeleton: The skeleton consists of tetractines and triactines, to which trichoxea-like diactines might be added (Fig. 5d). Triactines and the basal system of tetractines are lying tangentially within the tube wall in few layers (Fig. 5b, c). The apical actines of the tetractines protrude into the lumen of the tube (Fig. 5c). The diactines are arranged perpendicular to the tube walls with a broader tip in the sponge wall, and a trichoxea-like extension pointing outwards (Fig. 5a). They occur in the walls of external tubes and less frequently in the walls of internal tubes.

Spicules: *Triactines:* Equiradiate, equiangular. They have conical actines with blunt tips (Fig. 5d). Triactine dimensions of the holotype (SMF11627) are: 83–101.9 (SD 7.3)–116 μm × 11–13.1 (SD 1.2)–16 μm ($n = 20$). Spicule dimensions of the paratypes are provided in Table 2.

Tetractines: With basal system of similar size and shape as the triactines. The apical actine is usually thinner and can be shorter or longer than the basal actines. Tetractine dimensions of the holotype (SMF11627) are: Basal actines: 76–97.5 (SD 8.3)–114 μm × 10–12.4 (SD 1.1)–15 μm ($n = 20$); apical

Fig. 5 *Ernstia arabica* sp. nov. (OTU 2) **a** Holotype (SMF11627) *in situ*. **b** Section through external tubes (SMF11627). Arrows point at perpendicular diactines. **c** Section through tube wall showing the asconoid aquiferous system and the apical actine protruding into the tube's lumen (SMF11627). **d** Spicules (SMF11627): Triactines, tetractines, and diactines (description: see text). **e** Localities of collected specimens. dia = diactines, tetr = tetractine, tria = triactines

Table 2 Spicule sizes of *Ernstia arabica* sp. nov

Spicule type Specimen	Actine length in µm				Actine width in µm				Mean length/width	n
	Min	Mean	SD	Max	Min	Mean	SD	Max		
Triactines										
SMF11627*	83	101.9	7.3	116	11	13.1	1.2	16	7.8	20
Porifera-KAUMM-7	38	89.5	14.2	110	4	10.9	2.2	13	8.4	20
Porifera-KAUMM-8	62	86.1	10.4	102	9	12.8	1.6	15	6.8	20
combined	**38**	**92.5**	**12.9**	**116**	**4**	**12.2**	**2.0**	**16**	**7.7**	**60**
Tetractines (basal actines)										
SMF11627*	76	97.5	8.3	114	10	12.4	1.1	15	7.9	20
Porifera-KAUMM-7	57	88.6	13.0	110	10	11.6	2.2	14	7.7	20
Porifera-KAUMM-8	55	88.8	12.0	111	11	13.2	1.1	16	6.8	20
combined	**55**	**91.6**	**12.0**	**114**	**10**	**12.4**	**1.2**	**16**	**7.4**	**60**
Tetractines (apical actines)										
SMF11627*	56	98.2	26.0	156	6	7.9	0.8	10	12.4	13
Trichoxea-like diactines										
SMF11627*	196	351.8	112.3	480	2	4.0	1.4	6	88.0	9
Porifera-KAUMM-7	no diactines found									
Porifera-KAUMM-8	no diactines found									

(Min minimum, *SD* standard deviation, *Max* maximum). Mean values are underlined; n gives the number of measured spicules. * = Measurements of the holotype

actines: 56–98.2 (SD 26)–156 µm × 6–7.9 (SD 0.8)–10 µm (*n* = 13). Spicule dimensions of the paratypes are provided in Table 2.

Trichoxea-like diactines: If present, the trichoxea-like diactines are straight or slightly bent and are most wide near their proximal conical tip, from which the diameter continuously decreases to the trichoxea-like distal end. In the distal parts, the thin diactines can be slightly undulated. Diactine dimensions of the holotype (SMF11627) are: 196–351.8 (SD 112.3)–480 µm × 2–4.0 (SD 1.4)–6 µm (*n* = 9). Trichoxea-like diactines are missing in the paratypes.

Ecology: Most specimens were found in shallower depth between 0.5 to 8 m on hard substrate: under coral rubble on reef tops, or under overhangs.

Distribution: The distribution of the sampled specimens ranged from Dahab, Gulf of Aqaba in the north, to the Farasan Islands in the south (Fig. 5e). The species was not found between Duba and the Farasan Islands.

Remarks: In our phylogeny, *E. arabica* sp. nov. falls in one clade with *Ernstia tetractina* (Klautau and Borojević, 2001) and two undetermined "*Clathrina*" species, which probably belong to *Ernstia* (Fig. 2). Nine species are currently recognized in the genus (Van Soest et al. 2016). Three of these were reported to be yellow in life: *Ernstia chrysops* Van Soest and DeVoogd, 2015, *Ernstia klautauae* Van Soest, and DeVoogd, 2015, *Ernstia naturalis* Van Soest and DeVoogd, 2015 from Indonesia (Van Soest and De Voogd 2015). Of these, only *E. chrysops* contains diactines, but its cormus is only loosely anastomosed and the triactines and diactines are

more than twice the size of the spicules of *E. arabica* sp.nov. From all these species, *E. arabica* sp. nov. differs considerably in the shape of the tri- and tetractines as it becomes apparent when comparing the mean length/width ratio of the actines of the triradiate system, which is much smaller in *E. arabica* sp. nov.: Triactines: *E. chrysops:* 15.2 *E. klautauae*: 12.3; *E. naturalis:* 11.8; *E. arabica*: 7.8 in holotype (7.7 mean of measured specimens) ; tetractines: *E. chrysops*: 14.2 *E. klautauae*: 13.5; *E. naturalis*: 12.6; *E. arabica*: 7.9 in holotype (7.4 mean of measured specimens). Triactine length/width ratios in other *Ernstia* species according to the dimensions provided in the species descriptions range from 9.8 in *Ernstia quadriradiata* (Klautau and Borojević, 2001) to 11.9 in *Ernstia indonesiae* Van Soest and DeVoogd, 2015, tetractine ratios from 9.0 in *E. quadriradiata* to 12.3 in *Ernstia sepentrionalis* (Rapp, Klautau and Valentine, 2001).
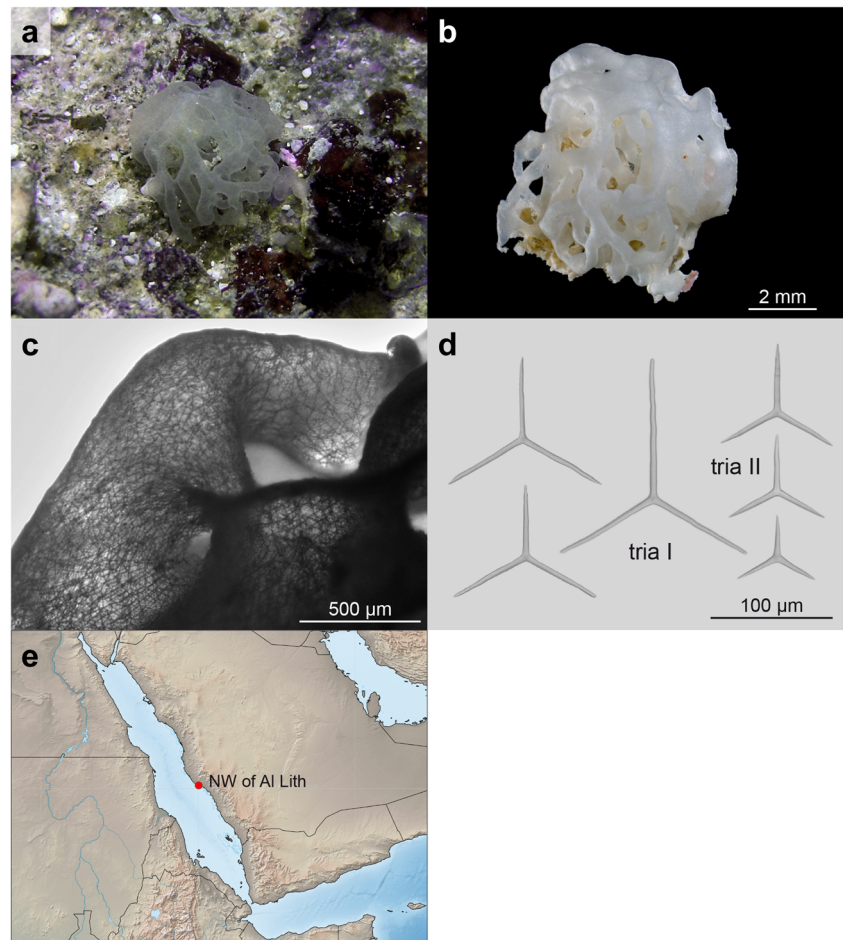
Genus *Clathrina* Gray, 1867

Diagnosis: "Calcinea in which the cormus comprises anastomosed tubes. A stalk may be present. The skeleton contains regular (equiangular and equiradiate) and/or parasagittal triactines, to which diactines and tripods may be added. Asconoid aquiferous system." (Klautau et al. 2013).

Clathrina rotundata sp. nov. Voigt, Erpenbeck and Wörheide

(Figure 6a-e, Suppl. Fig. 3).

Diagnosis: White *Clathrina* with a cormus of loosely anastomosed tubes, not growing on a peduncle. The skeleton consists of equiradiate to parasagittal triactines with cylindrical,

Fig. 6 *Clathrina rotundata* sp. nov. (OTU 4). **a** Specimen SMF11636 *in situ*. **b** Fixed specimen SMF11636. **c** Detail of the tube wall skeleton (SMF11636). **d** Spicules (SMF11636): equiradate triactines, parasagittal triactine (tria I), three sharp-tipped triactines (tria II). **e** Type locality. tria = triactine

sometimes slightly undulated actines with rounded tips, and smaller equiradiate triactines with conical to cylindrical, sharp-tipped actines.

Type Material: Holotype SMF11636.

Etymology: Latin *rotundata* (=rounded). Named for the rounded tips of spicules.

Material examined: 1 specimen: SMF11636.

Type locality: NW of Al Lith, Saudi Arabia: N20.19959° E40.04422°, 8 m depth, coll. O. Voigt, 3 March 2012.

Colour: White in life and in 80% ethanol.

OTU (C-region): OTU 4 ($n = 1$).

Growth form: The holotype has a clathroid cormus, about $7 \times 7 \times 3$ mm, consisting of loosely anastomosed tubes between ca. 300 and 800 μm in diameter (Fig. 6a, b). Oscula are not visible in the fixed specimen (Fig. 6b). The cormus is attached to the substrate and was not growing on a peduncle (Fig. 6a).

Skeleton: The tube wall is supported by overlapping triactines of two types (see below, Fig. 6c).

Spicules: *Triactine I:* Large equiradiate to parasagittal triactines, with cylindrical actines ending in rounded tips (Fig. 6d). Equiradiate triactines are much more frequent than parasagittal triactines. The unpaired actines of parasagittal triactines are longer or, less often, shorter than the paired actines. The triactines are often slightly undulated towards their distal tips (Fig. 6d). Triactine dimensions of these spicules are: 56–<u>86.8</u> (SD 15.9)–123 μm × 5–<u>5.7</u> (SD 0.4)–7 μm ($n = 20$).

Triactine II: Equiradiate triactines, with conical to cylindrical actines ending in sharp-pointed tips. These triactines are smaller than the round-tipped triactines, but can have wider actines (Suppl. Fig. 3). Dimensions of the sharp-tipped triactines are 15–<u>44.3</u> (SD 12.7)–73 × 4–<u>6.0</u> (SD 0.8)–8.

Ecology: The specimen was growing below a larger piece of coral rubble, in absence of direct sunlight.

Distribution: The type locality at the coast of Saudi Arabia, north west of Al Lith (Fig. 6e), is the only record for this species.

Remarks: In contrast to most other species observed here, there is no clear correlation between actine length and actine width of the rounded-tipped triactines (Suppl. Fig. 3). It seems that the growth of these triactines does not involve a secondary thickening by the so-called thickener cells, but only is driven by actine elongation by the founder cells, which promotes the tip growth of the spicules (Minchin 1908).

Clathrina rotundata is very closely related to *Clathrina blanca* (Miklucho-Maclay, 1868) (described from the Atlantic and also occurring in the Mediterranean Sea,

Imešek et al. 2013) and *C. ramosa* from the Pacific coast of Chile (Azevedo et al. 2009) according to our LSU and ITS phylogenies (Fig. 2, Suppl. Fig. 1), and it is also morphologically very similar regarding spicule types and sizes. However, both species were described to be growing on a peduncle, in which the parasagittal triactines occur (Azevedo et al. 2009; Imešek et al. 2014). Another very similar species is *Clathrina hispanica* Klautau, 2003 from the Mediterranean, which like *C. rotundata* sp. nov. does not have a peduncle (Klautau and Valentine 2003). Morphologically, *C. rotundata* sp. nov. differs from *C. hispanica* by the presence of parasagittal spicules that occur in the tube wall, not in a peduncle, and the occurrence of sharp-tipped triactines. Our analyses of ITS shows that *C. rotundata* sp. nov. is genetically distinct from all three species and is the sister taxon to all of them (Suppl. Fig. 1).

Clathrina sinusarabica Klautau and Valentine, 2003 (Figure 7a-d, Table 3, Suppl. Fig. 4).

Material examined: 5 specimens: SMF11631, Porifera-KAUMM-5, SNSB-BSPG GW3072, SNSB-BSPG GW3143, SMF11630.

Localities: SNSB-BSPG GW3072: Thuwal Reefs, Shi'b Nazar South, Saudi Arabia: N22.319033° E38.854383°, 10–25 m depth, coll. G. Wörheide, 25 April 2013; SNSB-BSPG GW3143: Thuwal Reefs, Palace Reef North, Saudi Arabia: N22.305447° E38.962214°, 10–25 m depth, coll. G. Wörheide, 28 April 2013; SMF11631: N of Qunfudhah, Saudi Arabia: N19.194762° E41.038531°, 8 m depth, coll. O. Voigt, 2 March 2012; Porifera-KAUMM-5, SMF11630: Reef SW of Qunfudhah, Saudi Arabia: N19.04472° E41.037°, both 15 m depth, coll. O. Voigt, 1 March 2012.

Colour: White in life and in 80% ethanol.

OTU (C-region): OTU 5, sequence identity 99.5% ($n = 5$).

Growth form: Clathroid cormi (SMF11631: 0.6 × 1.3 cm) of loosely anastomosed tubes with varying sizes (SMF11631: 0.3–1.0 mm in diameter), which reunite to one or several oscula (SMF11631: 0.7–1 mm in diameter) (Fig. 7a, Suppl. Fig. 4).

Aquiferous system: Asconoid.

Skeleton: Triactines are forming the skeleton of the tube walls (Fig. 7b).

Spicules: Triactines are equiangular, equiradiate, or rarely parasagittal with a shorter unpaired actine (Fig. 7c). The actines are straight, conical, and sharp-tipped. Triactine dimensions are: 51–112.8 (SD 22.8)–166 μm × 8–12.3 (SD 1.9)–18 μm (combined from five specimens, $n = 110$, Table 3).

Ecology: *Clathrina sinusarabica* was found in 8 to ca. 25 m depth, growing on hard substrate on reef walls, under overhangs, in cracks, sometimes alongside with other sponges.

Distribution: In this work, specimens were found at reefs near Thuwal and Qunfudhah, Saudi Arabia (Fig. 7d). The only other record is the holotype (1 specimen), which was sampled near Suez (Row 1909; Klautau and Valentine 2003).

Remarks: Klautau and Valentine (2003) described *Clathrina sinusarabica* from material of the Crossland collection, which previously was referred to as *Clathrina coriacea* (Montagu, 1818) by Row (1909). According to the species description of *C. sinusarabica*, the main morphological differences to several other species of *Clathrina* are the shape and size of the triactines. Genetically, we here document a close relationship to *C. luteoculcitella* Wörheide and Hooper, 1999, described from the Great Barrier Reef, to a specimen described as *Clathrina* aff.
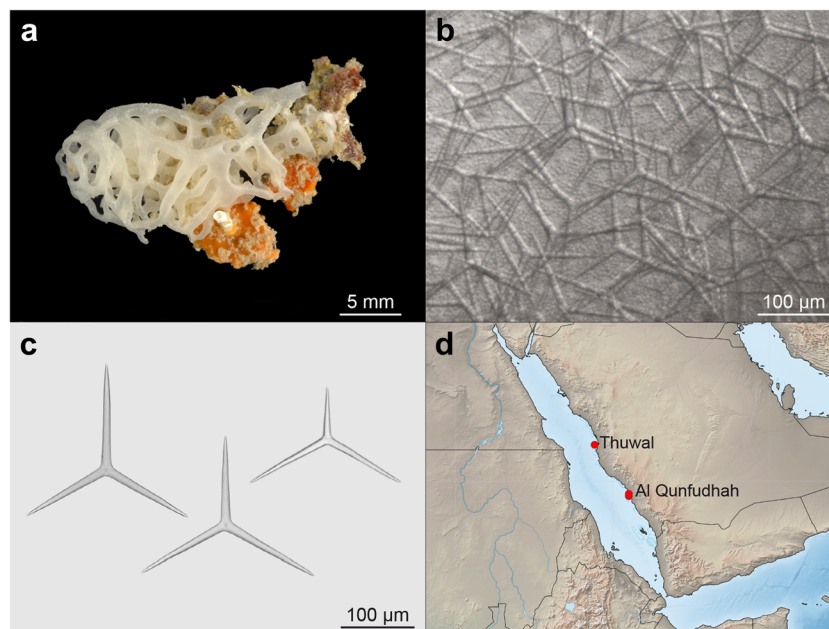

Fig. 7 *Clathrina sinusarabica* (OTU 5). **a** Specimen SMF11631 before fixation. **b** Detail of the tube wall skeleton (SMF11631). **c** Spicules (SMF11631): Two equiradiate triactines and one rare parasagittal triactine. **d** Localities of collected specimens

Table 3　Triactine sizes of *C. rowi* sp.nov. and *C. sinusarabica*

Species	Specimen	Actine length in μm				Actine width in μm				Mean length/width	n
		Min	Mean	SD	Max	Min	Mean	SD	Max		
Clathrina rowi sp. nov.											
	SMF11632*	37	<u>79.4</u>	12.1	99	8	<u>10.0</u>	1.1	13	8.0	20
	SMF11532	69	<u>85.3</u>	6.0	99	9	<u>10.3</u>	0.8	13	8.3	20
	SMF11633	65	<u>80.7</u>	7.4	97	8	<u>10.5</u>	1.0	13	7.7	20
	Porifera-KAUMM-2	51	<u>71.1</u>	11.1	101	6	<u>8.9</u>	1.0	11	8.0	20
	SMF11629	60	<u>87.9</u>	7.9	103	8	<u>10.2</u>	0.8	12	8.7	20
	SMF11634	34	<u>70.3</u>	14.1	88	7	<u>9.0</u>	0.9	11	7.8	20
	combined	**34**	**<u>79.1</u>**	**12.0**	**103**	**6**	**<u>9.8</u>**	**1.1**	**13**	**8.1**	**120**
Clathrina sinusarabica											
	BMNH 1912.2.1.1*	72	<u>91.9</u>	9.1	103	–	<u>8.4</u>	1.0	–	10.9	20
	SMF11630	62	<u>99.4</u>	14.1	126	8	<u>10.6</u>	1.2	13	9.5	20
	SMF11631	51	<u>95.5</u>	21.4	137	8	<u>10.9</u>	1.1	13	8.7	20
	Porifera-KAUMM-5	66	<u>111.6</u>	17.6	139	9	<u>12.8</u>	1.2	15	8.8	30
	SNSB-BSPG GW3072	71	<u>137.8</u>	19.4	166	12	<u>14.7</u>	1.5	18.	9.4	20
	SNSB-BSPG GW3143	81	<u>119.3</u>	16.2	153	10	<u>12.3</u>	1.3	15	9.7	20
	combined (excluding holotype)	**51**	**<u>112.8</u>**	**22.8**	**166**	**8**	**<u>12.3</u>**	**1.9**	**18**	**9.2**	**110**

(*Min* minimum, *SD* standard deviation, *Max* maximum). Mean values are underlined; n gives the number of measured spicules. * = Measurements of the holotypes. Measurements of BMNH 1912.2.1.1 by Klautau and Valentine (2003)

luteoculcitella from Indonesia (Van Soest and De Voogd 2015) and *Clathrina rowi* sp. nov. (OTU 6, see below) from the Red Sea (Fig. 2, Suppl. Fig. 1). *Clathrina luteoculcitella* and *C.* aff. *luteoculcitella* differ from *C. sinusarabica* by being (pale) yellow in life, by having smaller triactines (mean: 77.7 μm × 9.4 μm in *C. luteoculcitella,* Wörheide and Hooper 1999), and by possessing diactines. The two Red Sea species *C. sinusarabica* and *C. rowi* nov. sp. (see below) can be distinguished by 14 synapomorphic substitutions in their LSU C-region sequences. The intraspecific variation of both species is much lower (Suppl. Fig. 5). In addition to the genetic differences, *C. sinusarabica* and *C. rowi* sp. nov. also differ regarding the appearance of the cormus and the size of the triactines, which are larger in *C. sinusarabica* (Table 3). The spicule sizes in the studied specimens were quite variable, and on average larger than in the holotype (Table 3). Compared to *Clathrina rowi* sp. nov. (see below), the average actine length/width ratio of our specimens of *C. sinusarabica* (9.2) was smaller than in the holotype (10.9), but still larger than in *C. rowi* sp. nov. (8.1, see Table 3 for all values). Some specimens of *C. sinusarabica* and *C. rowi* sp. nov. were sampled at the same localities.

Clathrina rowi sp. nov. Voigt, Erpenbeck and Wörheide (Figure 8a-f, Table 3, Suppl. Fig. 6)

Diagnosis: White *Clathrina* with cormi formed of more densely anastomosed tubes of varying diameter, which re-unite as water-collecting tubes to one or several oscula that have a larger diameter than the majority of the tubes. The skeleton is made from triactines, which vary from equiangular

and equiradiate spicules to parasagittal triactines with shorter unpaired actines. The actines of triactines are cylindrical and sharp-tipped and only rarely exceed a length of 100 μm. Trichoxea-like diactines may be present.

Type Material: Holotype SMF11632

Additional material: Paratypes: Porifera-KAUMM-3, SMF11633, SMF11634, Porifera-KAUMM-2, SMF11532, SMF11629, Porifera-KAUMM-4, SMF11507

Etymology: Named after R. W. Harold Row (1840–1919) in recognition of his taxonomic work on Red Sea calcareous sponges.

Type locality: SMF11632**:** N of Qunfudhah, Saudi Arabia: N19.194762° E41.038531°, 8 m depth, coll. O. Voigt, 2 March 2012.
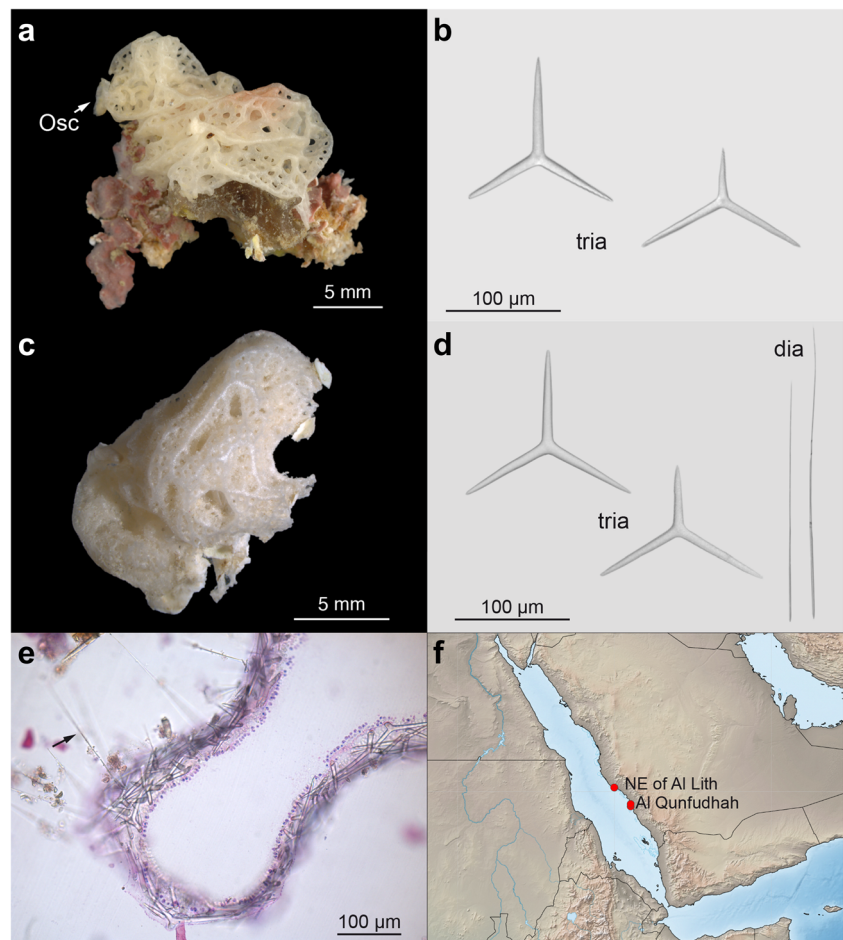
Additional localities: SMF11634: NE of Al Lith, Saudi Arabia, N20.25358° E39.98969°, <0.5 m depth, coll. O. Voigt, 6 March 2012; SMF11633: NE of Al Lith, Saudi Arabia, N20.245417° E40.00095°, ca. 10 m depth, coll. O. Voigt, 5 March 2012; SMF11507, SMF11532, SMF11629, Porifera-KAUMM-2, Porifera-KAUMM-3, Porifera-KAUMM-4: Reef SW of Qunfudhah, Saudi Arabia: N19.04472° E41.037°, all between 15 and 18 m, coll. O. Voigt, 1 March 2012.

Colour: White in life and in 80% ethanol.

OTU (C-region): OTU 6, sequence identity 99.5% (*n* = 9).

Growth form: Clathroid cormi (in the holotype: 1.6 × 0.9 cm) of more densely anastomosed tubes of varying sizes (in the holotype: 0.3–0.7 mm). The anastomosis results in rounded spaces between the tubes, giving the cormus a

Fig. 8 *Clathrina rowi* sp. nov.
(OTU 6). **a** Holotype SMF11632
before fixation (Osc = osculum).
b Spicules of SMF11632:
equiangular and equiradiate
triactine, rare parasagittal
triactine. **c** SMF11633, fixed
specimen with trichoxeas, which
trap detritus between the tubes. **d**
Spicules of SMF11633:
equiangular and equiradiate
triactines, rare parasagittal
triactine and trichoxea-like
diactines. **e** Section through tube
wall of specimen SMF11633,
showing the asconoid aquiferous
system, the arrow points at one
of the numerous perpendicular
trichoxea-like diactines that are
present in this specimen. **f**
Localities of collected specimens.
dia = diactines, tria = triactines

mesh-like appearance. One or few oscula are present, with a
much larger diameter than the tubes (e.g. in the holotype:
3.5 mm). Oscula are often collapsed in the fixed specimens
(Fig. 8a, c, Suppl. Fig. 6).

Aquiferous system: Asconoid.

Skeleton: Triactines are forming the skeleton of the tube
walls. One specimen (SMF11633) contained many diactines,
arranged perpendicular in the sponge wall, pointing outwards.
These were most common on the outer tubes, less common on
internal tubes.

Spicules: *Triactines:* Equiangular, equiradiate or
parasagittal with a shorter unpaired actine (Fig. 8b, d). The
actines are conical and blunt-tipped. Triactine dimensions of
the holotype (SMF11632): 37–79.4 (SD 12.1)–99 μm × 8–
10.0 (SD 1.1)–13 μm (*n* = 20). For triactine dimensions of
additional specimens, see Table 3.

Trichoxea-like diactines: Trichoxea-like diactines are pres-
ent in specimen SMF11633 (Fig. 8c). They are straight and
most wide near their proximal conical tip. From there, the
diameter continuously decreases to the trichoxea-like distal
end, which can be slightly undulated (Fig. 8d, e). Diactine
dimensions in specimen SMF11633 are: 184–219.1 (SD
24.3)–261 μm × 1–1.9 (SD 0.3)–2.4 μm (*n* = 10).

Ecology: *Clathrina rowi* sp. nov was found from reef flats
(<0.5 m) until 18 m depth. It was growing on hard substrate,
on reef walls, under reef overhangs and in cracks, and under
coral rubble, sometimes along side with other sponges.

Distribution: Specimens in the collections are from the
Saudi Arabian coast of the southern Red Sea, near Al Lith
and Qunfudhah (Fig. 8f).

Remarks: Trichoxea-like diactines are absent in most
specimens, but very frequent in specimen SMF11633. The
presence/absence of diactines therefore seems to be no diag-
nostic character for *C. rowi* sp. nov. The species is genetically
very similar to *C. sinusarabica* (see above for details), and
C. luteoculcitella (see above). From the latter it can be easily
distinguished by the white life colour (*C. luteoculcitella* is
yellowish). The genetic differences between the Red Sea spe-
cies *Clathrina rowi* sp. nov. and *C. sinusarabica* were already
mentioned above. Morphologically, the two species differ re-
garding the appearance of the cormus, and the size of the
triactines, which are on average smaller in *C. rowi* sp. nov.
(Table 3). The actine length/width ration is on average also
smaller in *C. rowi* sp. nov. compared to *C. sinusarabica* (8.1
vs. 9.2, respectively, Table 3); however, it also can get very
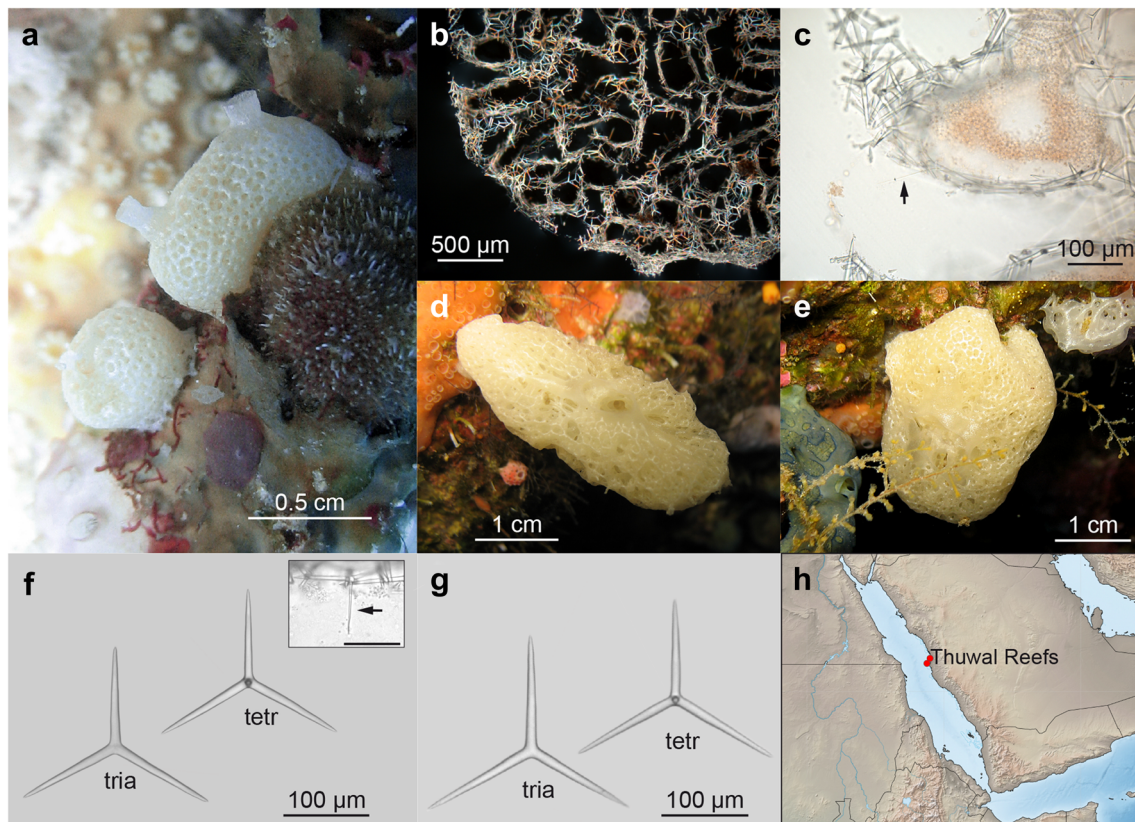similar in some specimens.

Fig. 9 *Arthuria sueziana* (OTU7). **a** Specimen SNSB-BSPG GW3168 *in situ*. **b** Section (specimen SNSB-BSPG GW3168): overview of skeleton. **c** Detail of section, showing the skeletal organization. The arrow points at of the rare trichoxeas, which were not detected in the spicule preparations. **d** Specimen SNSB-BSPG GW3120 *in situ*. **e** Specimen SNSB-BSPG GW3121 *in situ*. **f** Spicules of specimen SNSB-BSPG GW3168: Triactine and tetractine, inset: arrow points at apical actine of a tetractine protruding to the tube's lumen (scale 100 μm). **g** Spicules of specimen SNSB-BSPG GW3120: Triactine and tetractine. **h** Localities of collected specimens. tetr = tetractine, tria = triactines

Genus *Arthuria* Klautau, Azevedo, Cóndor-Luján, Rapp, Collins, and Russo, 2013

Diagnosis: "Calcinea in which the cormus comprises a typical clathroid body. A stalk may be present. The skeleton contains regular (equiangular and equiradiate) triactines and tetractines. However, tetractines are more rare. Diactines may be added. Asconoid aquiferous system." (Klautau et al. 2013).

Arthuria sueziana (Klautau and Valentine, 2003)

(Figure 9a-h, Table 4, Suppl. Table 2) (Table 5).

Synonymised names: *Clathrina canariensis var. compacta* sensu Row, 1909, *Clathrina compacta sensu* Row, 1909 (not (Schuffner, 1877)), *Clathrina sueziana* Klautau and Valentine 2003.

Material examined: 3 specimens: SNSB-BSPG GW3120, SNSB-BSPG GW3121, SNSB-BSPG GW3168.

Localities: SNSB-BSPG GW3120, SNSB-BSPG GW3121: Thuwal Reefs, Saudi Arabia: N22.432661° E38.993297°, 10–25 m depth, coll. G. Wörheide, 27 April 2013; SNSB-BSPG GW3168: Thuwal Reefs, Saudi Arabia N22.062093° E38.763701°, 10–25 m depth, coll. G. Wörheide, 29 April 2013.

Colour: Beige in life and in 80% ethanol.

OTU (C-region): OTU 7, sequence identity 100% ($n = 3$).

Growth form: Globular clathroid sponges with densely anastomosing tubes, the cormi are between 0.5 and 2.5 cm in diameter (Fig. 9a-e). The specimens have water-collecting tubes ending in large oscula (one or two, Fig. 9a, d, e).

Aquiferous system: Asconoid.

Skeleton: Triactines and tetractines (Fig. 9f, g) form the skeleton of the tube-wall, the apical actine of the tetractines reach inside the tube's lumen (Fig. 9b). Rare perpendicular trichoxea-like diactines were observed in sections to point outwards from the exterior tube walls (Fig. 9c).

Spicules: *Triactines:* Equiradiate, equiangular, with conical actines and blunt tips (Fig. 9f, g). Triactine dimensions are (combined from the three specimens, Table 4): 64–99.4 (SD 19.9)–140 μm × 6–10.8 (2.3)–15 μm ($n = 60$).

Tetractines: Basal system equiradiate, equiangular, actines are of similar form and shape as the triactines. The apical actines are about half the thickness of the basal actines, but of similar length (Fig. 9f, inset). Tetractine dimensions are: basal system (combined from the three specimens, Table 4):

Table 4 Spicule sizes of *A. sueziana*

Spicule type	Specimen	Actine length in μm				Actine width in μm				Mean length/width	n
		Min	Mean	SD	Max	Min	Mean	SD	Max		
Triactines											
	SNSB-BSPG GW3120	88	116.4	10.2	140	8	11.6	1.7	14	10.1	20
	SNSB-BSPG GW3121	64	74.3	5.3	89	6	7.9	0.7	10	9.4	20
	SNSB-BSPG GW3168	87	107.5	8.5	121	11	13.1	0.8	15	8.3	20
	combined	**64**	**99.4**	**19.9**	**140**	**6**	**10.8**	**2.3**	**15**	**9.2**	**60**
	BMNH 1912.2.1.3*	75	91.3	10.9	138	–	10.3	1.5	–	8.9	30
Tetractines (basal actines)											
	SNSB-BSPG GW3120	103	114.4	8.3	130	9	10.7	0.9	12	10.1	5
	SNSB-BSPG GW3121	49	73.8	8.7	91	6	7.8	0.7	9	9.5	20
	SNSB-BSPG GW3168	84	109.9	10.6	127	10	12.3	1.1	16	9.0	15
	combined	**49**	**92.2**	**20.9**	**130**	**6**	**9.8**	**2.3**	**16**	**9.4**	**40**
	BMNH 1912.2.1.3*	70.0	86.0	6.1	98	–	9.4	1.4	–	9.1	30
Tetractines (apical actines)											
	SNSB-BSPG GW3168	70	102.1	13.9	118	4	6.2	1.5	8	16.6	14
	BMNH 1912.2.1.3*	50	56.3	4.5	63	–	5.0	–	–	–	4
Trichoxea-like diactines											
	SNSB-BSPG GW3168	–	>130	–	–	–	2.0	–	–	–	1
	BMNH 1912.2.1.3*	–	>250	–	–	–	<0.3	–	–	–	–

(*Min* minimum, *SD* standard deviation, *Max* maximum). Mean values are underlined; n gives the number of measured spicules. * = Measurements of the holotype of *A. sueziana* (BMNH 1912.2.1.3) from Klautau and Valentine (2003)

49–92.2 (SD 20.9)–130 μm × 6–9.8 (SD 2.3)–16 (*n* = 40); apical actines (measured in sections of specimen SNSB-BSPG GW3168): 70–102.1 (SD 13.9)–118 μm × 3.6–6.0 (SD 1.5)–8 μm (*n* = 14).

Trichoxeas: Trichoxeas are thin and were only observed in sections of specimen SNSB-BSPG GW3168 (Fig. 9c). Detailed spicule dimensions are, therefore, not available (trichoxea in Fig. 9c: ca. 2 μm wide, longer than 130 μm).

Ecology: The specimens were growing under overhangs on hard substrate and did not receive direct sunlight.

Distribution: In this work, specimens were only found at reefs near Thuwal, Saudi Arabia (Fig. 9h). The only other report (1 specimen) is the type locality, Suez, Egypt (Row 1909).

Remarks: No other LSU sequence is yet available for the genus *Arthuria*. According to ITS data, *A. sueziana* is the sister taxon to *Arthuria hirsuta* (Klautau and Valentine, 2003), the type

Table 5 Spicule sizes of *B.* aff. *aspina* and *B. aspina*

Spicule type	Specimen	Actine length in μm				Actine width in μm				Mean length/width	n
		Min	Mean	SD	Max	Min	Mean	SD	Max		
Triactines											
	SMF11637	48	79.6	11.9	106	7	10	1.1	13	7.9	50
	B. aspina planar triactines*	55	70.0	7.5	80	–	6.0	1.0	–	11.7	30
	B. aspina tripods*	63	78.8	8.8	93	–	9.5	0.8	–	8.3	30
Tetractines (basal actines)											
	SMF11637	48	69.7	8.1	85	7	9.1	1.2	11	9.1	14
	*B. aspina**	53	68.8	7.8	83	–	6.0	1.0	–	11.5	30
Tetractines (apical actines)											
	SMF11637	46	68.6	16.5	98	5	6.9	1.0	8	9.9	8
	*B. aspina**	40	50.3	6.3	63	–	5.0	0.0	–	10.1	30

(*Min* minimum, *SD* standard deviation, *Max* maximum). Mean values are underlined; n gives the number of measured spicules. * = Measurements of *B. aspina* from Klautau and Valentine (2003)

species of the genus (Suppl. Fig. 1). *Arthuria sueziana* is morphologically very similar to *Arthuria tenuipilosa* (Klautau and Valentine 2003), which was described from the Indian Ocean, Gulf of Mannar (Dendy 1905) and also occurs in the Red Sea (Row 1909). Klautau and Valentine (2003) differentiated the two species by the presence of water-collecting tubes in *A. sueziana*, which are lacking in *A. tenuipillosa*. They also reported less frequent trichoxeas in *A. sueziana* and a thinner diameter of the apical actines in the tetractines. Unfortunately, Row (1909) did not describe the Red Sea specimens of *A. tenuipilosa*. Spicule sizes of these two species are very similar (Suppl. Table 2). An additional species that has been reported from the Red Sea is *Arthuria darwini* (Haeckel, 1870), which like *A. tenuipilosa* lacks collecting tubes (Haeckel 1872). Our decision to identify our specimens as *A. sueziana* is based on the presence of the water-collecting tubes.

Genus *Borojevia* Klautau, Azevedo, Cóndor-Luján, Rapp, Collins and Russo, 2013

Diagnosis: "Calcinea in which the cormus comprises tightly anastomosed tubes. The skeleton contains regular (equiangular and equiradiate) triactines, tetractines, and tripods. The apical actine of the tetractines has spines. Aquiferous system asconoid." (Klautau et al. 2003).

Remarks: The spines of apical actines are not always present. The original description of *Borojevia aspina* (Klautau, Solé-Cava and Borojević, 1994) explicitly mentions the absence of these spines (Klautau et al. 1994), although later works report 'occasional' vestigial spines (Klautau and Valentine 2003).

Borojevia aff. *aspina* Klautau, Solé-Cava and Borojević, 1994

(Figure 10a-g, Suppl. Fig. 7, Table 5)

Material examined: SMF11637, Porifera-KAUMM-1.

Localities: SMF11637: NE of Al Lith, Saudi Arabia, N20.19959° E40.04422°, 8 m depth, coll. O. Voigt, 7 March, 2012; Porifera-KAUMM-1: Reef SW of Qunfudhah, Saudi Arabia: N19.04472° E41.037°, ca. 15 m depth, coll. O. Voigt, 1 March 2012.

Colour: White in life and in 80% ethanol.

OTU (C-region): OTU 8, sequence identity 99.99% ($n = 2$).

Growth form: Flat, cushion-shaped cormi (SMF11637: ca. 10 mm × 5 mm) of tightly anastomosed tubes, ca. 200–300 μm in diameter, combining to one or few larger tubes ending with an osculum (SMF11637: ca. 1.4 mm). The spaces between the tubes have a round shape and are usually between 100 and 400 μm in diameter in specimen SMF11637 (Fig. 10a-c).

Aquiferous system: Asconoid.

Skeleton: Triactines and the basal triradiate system of tetractines support the tube walls; the apical actines of tetractines protrude into the lumen of the tubes (Fig. 10d, e). Triactines are more frequent than tetractines. Trichoxeas occur on the outer tubes, arranged perpendicular to the tube and

protruding the sponge walls. They were only observed in sections (Fig. 10d). Tripods, if present, must be very similar to triactines with their center only being slightly out of the planes of the actine tips. We could not with any certainty distinguish them from planar triactines.

Spicules: *Triactines:* Equiradiate triactines with conical actines and sharp tips (Fig. 10e). Tripods could not be unambiguously distinguished from them. Measurements of 50 randomly picked triactines seem to constitute one continuum of actine lengths and widths, which show a correlation (Suppl. Fig. 7). Triactine dimensions of specimen SMF11637 are: 48–79.6 (SD 11.9)–106 μm × 7–10.0 (SD 1)–13 μm ($n = 50$).
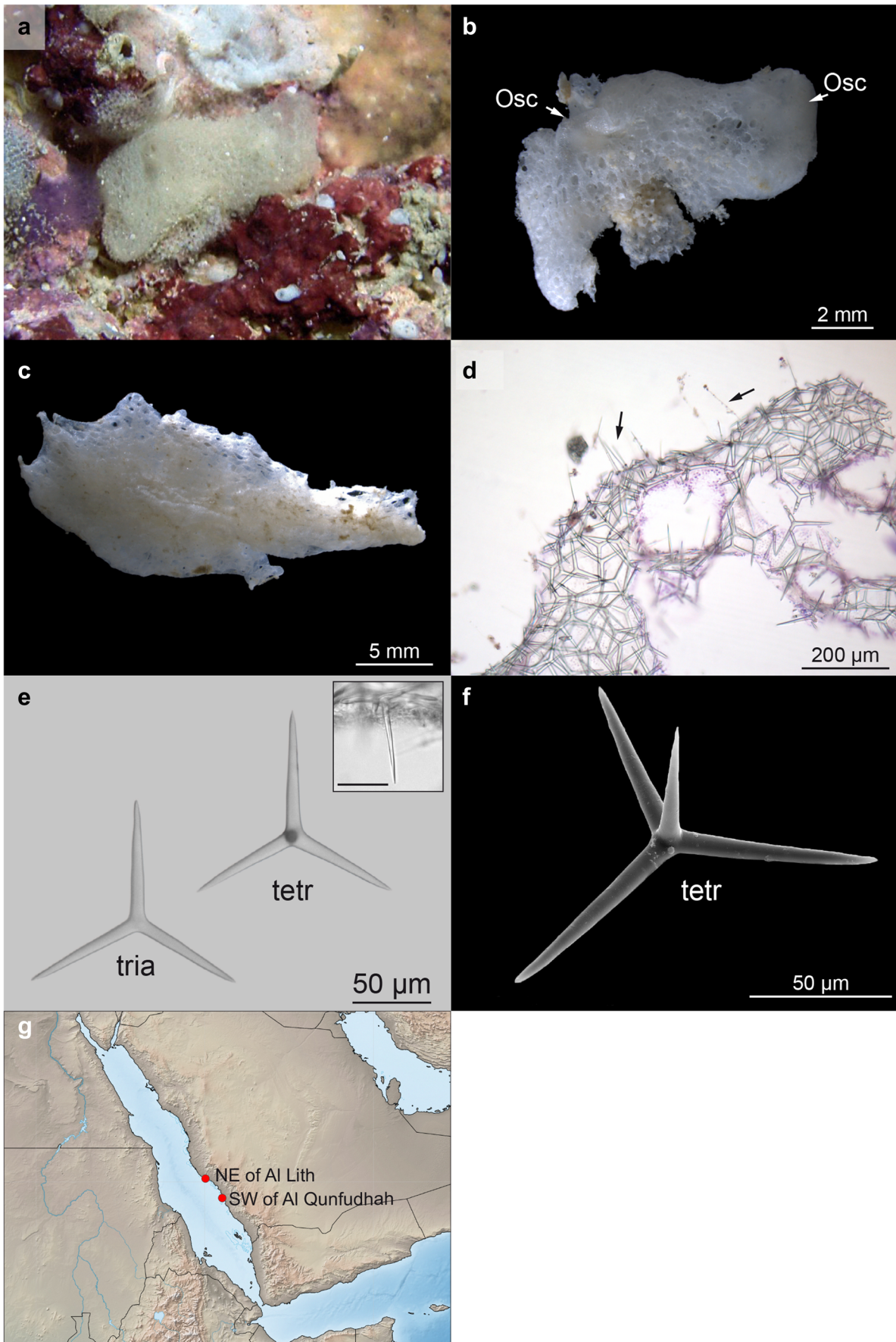
Tetractines: With a basal system of similar size and shape as the triactines (Fig. 10e, f). The apical actine is also conical and about as long as the actines of the basal system, and smooth. Spines on apical actines were not detected, also not by SEM inspection (Fig. 10f). Tetractine dimensions of specimen SMF11637 are: actines of the basal system: 48–69.7 (SD 8.1)–85 μm × 7–9.1 (SD 1.2)–11 μm (n = 14); dimensions of apical actines are: 46–68.6 (SD 16.5)–98 μm × 5–6.9 (SD 1.0)–8 μm ($n = 8$).

Trichoxeas: Very thin, their length is 108–141.4 (SD 19.3)–169 ($n = 7$).

Ecology: The specimens were growing under an overhang and beneath a larger piece of coral rubble, respectively, on hard substrate without direct sunlight.

Distribution: Middle/southern Red Sea coast of Saudi Arabia (NE of Al Lith and SW of Qunfudhah, Fig. 10g).

Remarks: *Borojevia* aff. *aspina* is very closely related to *Borojevia aspina* in the molecular phylogenies (Fig. 2, Suppl. Fig. 1). The C-region sequences of the two species are 99.5% identical. Our specimens and *B. aspina* have smooth apical tetractines, although in *B. aspina*, vestigial spines on the apical actines of tetractines occur "occasionally" (Klautau and Valentine 2003). The spicule sizes are very similar (Table 5), but in our specimens, we could not distinguish tripods from planar triactines. If they are present at all, they must have their centre only very slightly outside of the tips plane, and are not distinguishable from other triactines in spicule preparations regarding their size. This sometimes is also the case in *B. aspina* (Klautau and Valentine 2003). Indeed, all observed triactines show a continuous variation of width and length of their actines, but possibly very rare tripods were missed in our inspection (Suppl. Fig. 7). Moreover, the length/width ratio of our specimen's triactines is closer to *B. aspina* tripods than to its planar triactines (Table 5). Trichoxeas that we observed in our specimens were not reported for *B. aspina* or any other *Borojevia* species so far. It remains unclear if they do not occur in the other *Borojevia* species or were not mentioned because they were considered as "taxonomical unimportant". *Borojevia aspina* was described from the Atlantic coast of Brazil (Klautau et al. 1994). If our specimens are really con-specific, the distribution is very disjunct, or it can be expected to find *B. aspina* in other

◀ **Fig. 10** *Borojevia* aff. *aspina* (OTU 8). **a**, **b** Specimen SMF11637 *in situ* and fixed (Osc=osculum); **(c)** Specimen Porifera-KAUMM-1, fixed. **d** Section of specimen SMF11637, arrows point at perpendicular trichoxeas. **e** Triactine and tetractine (specimen SMF11637), inset: apical actine of tetractine (scale 50 μm). **f** SEM image of a tetractine (specimen SMF11637), showing the absence of spines on the apical actine. **g** Localities of collected specimens. tetr = tetractine, tria = triactine

regions, too. For now, we decided not to consider the Red Sea specimens as a new species due to the high sequence similarity.

Family Leucettidae de Laubenfels, 1936

Diagnosis: "Clathrinida with a solid body. The aquiferous system is always leuconoid. The choanoskeleton is well developed, in the form of a regular network composed of triactines and/or tetractines. The cortex is thin and composed of spicules similar to those of the choanoskeleton." (Borojević et al. 2002).

Genus *Leucetta* Haeckel, 1872

Diagnosis: "Leucettidae with a homogeneous organisation of the wall and a typical leuconoid aquiferous system. There is neither a clear distinction between the cortex and the choanoskeleton, nor the presence of a distinct layer of

subcortical inhalant cavities. The atrium is frequently reduced to a system of exhalant canals that open directly into the osculum." (Borojević et al. 1990).

Remarks: Molecular phylogenies repeatedly have shown that the genus is not monophyletic, and that some species of *Leucetta* are more closely related to species of *Pericharax* Poléjaeff, 1883 (e.g., Voigt et al. 2012a; Klautau et al. 2013; Voigt and Wörheide 2016). A revision of the two genera is necessary.

Leucetta chagosensis Dendy, 1913
(Figure 11a-d, Suppl. Fig. 8, Table 6)

Synonymised names: *Leucetta expansa* Row and Hozawa, 1931; *Leucetta infrequens* Row and Hozawa, 1931.
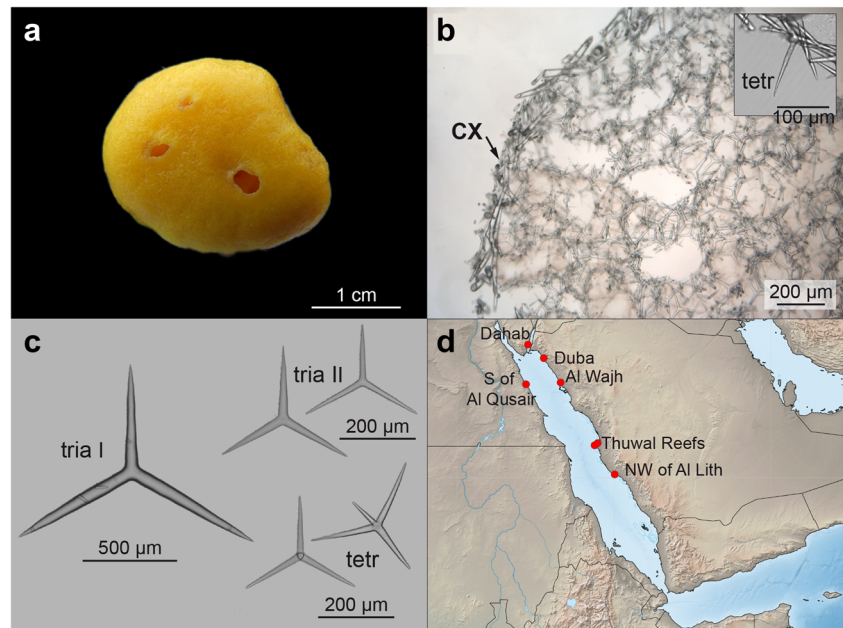
Material examined: Holotype BMNH 1920.12.9.51 (spicule preparation) "Sealark collection", Salomon (Chagos Archipelago); 11 specimens from the Red Sea: SNSB-BSPG GW1122, SNSB-BSPG GW2973, SNSB-BSPG GW3039, SNSB-BSPG GW3052, SNSB-BSPG GW3162, SNSB-BSPG GW3178, Porifera-KAUMM-9, Porifera-KAUMM-10, Porifera-KAUMM-11, SMF11598, SMF11635.

Table 6 Spicule sizes of *L. chagosensis*

Spicule type / Specimen	Actine length in μm				Actine width in μm				Mean length/width	n
	Min	Mean	SD	Max	Min	Mean	SD	Max		
Large cortical triactines										
Porifera-KAUMM-11	212	371.4	88.8	548	21	29.5	6.2	49	12.1	15
Porifera-KAUMM-9	279	373.9	70.8	481	26	39.3	7.0	48	12.1	5
Porifera-KAUMM-10	201	329.0	74.7	512	22	30.2	5.1	42	12.1	12
SMF11635	278	412.3	61.4	576	26	32.6	3.4	42	12.6	20
combined	**201**	**383.2**	**78.3**	**576**	**21**	**32.3**	**6.0**	**49**	**12.4**	**52**
BMNH 1920.12.9.51	about 590*				about 46*					
Small triactines										
Porifera-KAUMM-11	99	141.8	22.4	203	11	15.1	2.0	20	9.4	20
Porifera-KAUMM-9	81	143.6	25.6	190	9	15.2	3.3	22	9.7	23
Porifera-KAUMM-10	70	136.4	30.4	222	10	14.7	2.4	21	9.2	22
SMF11635	96	148.4	22.9	188	10	14.6	2.1	20	10.2	20
combined	**71**	**142.4**	**25.9**	**222**	**9**	**14.9**	**2.6**	**22**	**9.6**	**85**
BMNH 1920.12.9.51	99	170.8	30.6	210	9	15.3	2.0	19	11.2	20
	about 190*				about 17.4					
Tetractines (basal actines)										
Porifera-KAUMM-11	100	125.2	12.4	159	10	13.0	1.6	18	9.7	20
Porifera-KAUMM-9	92	116.9	12.6	143	9	11.9	1.5	16	9.9	20
Porifera- KAUMM-10	62	113.3	17.4	150	10	12.0	1.3	16	9.4	20
SMF11635	86	130.1	19.5	165	10	12.4	1.4	16	10.5	20
combined	**62**	**121.4**	**17.0**	**165**	**9**	**12.3**	**1.5**	**18**	**9.9**	**80**
BMNH 1920.12.9.51	90	123.2	16.9	168	8	11.2	1.5	15	11.0	19
Tetractines (apical actines)										
Porifera-KAUMM-9	61	86.7	24.4	125	7	8.3	1.0	10	10.3	5

(*Min* minimum, *SD* standard deviation, *Max* maximum). Mean values are underlined; n gives the number of measured spicules. * = Measurements of the holotype of *L. chagosensis* (BMNH 1920.12.9.51): * = Dendy (1913), otherwise own measurements

Fig. 11 *Leucetta chagosensis* (OTU 9). **a** Living specimen before fixation (Porifera-KAUMM-11). Section through sponge wall (Porifera-KAUMM-9), inset: apical actine of tetractine, protruding into the lumen of a canal. **c** Spicules (SNSB-BSPG GW1122): Large cortical triactines (tria I) and smaller triactines (tria II), tetractines (tetr). **d** Localities of of collected specimens. cx = cortex, tetr = tetractine, tria = triactine

Localities: SNSB-BSPG GW1122: Dahab, Egypt, N28.48000, E34.513000°, 0.5 m depth, coll. G. Wörheide, 28 September 2009; Porifera-KAUMM-11: Duba, Saudi Arabia, N27.618667° E35.519667°, coll. D. Erpenbeck, 19 June 2013; Porifera-KAUMM-9, Porifera-KAUMM-10, SMF11598: Al-Wajh, Saudi Arabia, N26.058278° E36.594725°, coll. D. Erpenbeck, 11 June 2013; SNSB-BSPG GW2973: S of Al Qusair, Egypt, N25.943031, E34.389128°, coll. G. Haszprunar at 5–10 m; SNSB-BSPG GW3039, SNSB-BSPG GW3052, Thuwal Reefs, Sodfa, Saudi Arabia N22.201194° E38.958722°, 9 m depth, coll. G. Wörheide, 24 April 2013; SNSB-BSPG GW3178: Thuwal Reefs, Abu Madafi centre, Saudi Arabia, N22.063362° E38.764187°,15 m depth, coll. G. Wörheide, 29 April 2013; SNSB-BSPG GW3162: Thuwal Reefs, Abu Madafi centre, Saudi Arabia, N22.062092° E38.763700°, 20 m depth, coll. G. Wörheide, 29 April 2013; SMF11635: Saudi Arabia, NW of Al Lith, N20.19959° E40.04422°, 8 m depth, coll. O. Voigt, 7 March 2012.

Colour: Yellow in life, white in 70–80% ethanol.

OTU (C-region): OTU 9, sequence identity 100% ($n = 11$).

Growth form: Massive, globular, or elongated-globular sponges of about 0.8 to 2.5 cm. The sponges have one or several large oscular openings of about 1.5 to 3 mm (Fig. 11a, Suppl. Fig. 8).

Aquiferous system: Leuconoid.

Skeleton: Two types of triactines: Large triactines and small triactines form the cortical skeleton (Fig. 11b). The choanosomal skeleton mainly consists of smaller triactines (Fig. 11b). Tetractines are less abundant and occur in the wall of (exhalant?) canals, with their basal system tangential in the canal walls and the apical actine protruding into the lumen of the canals (Fig. 11b, inset).

Spicules: *Triactines I:* Large cortical triactines are equiangular, equiradiate, with conical, sharp-tipped actines (Fig. 11c). Spicule dimensions are (combined from 4 specimens, Table 6): 201–<u>383.2</u> (SD 78.3)–576 μm × 21–<u>32.3</u> (SD 6.0)–49 μm ($n = 52$). Note that while single actines were shorter than the largest actines of the smaller triactines, all of the larger triactines had at least one actine that was longer than 260 μm.

Triactines II: Smaller triactines, equiangular and equiradiate, with conical, sharp-tipped actines (Fig. 11c). Spicule dimensions are (combined from 4 specimens, Table 6): 71–<u>142.4</u> SD (25.9)–222 μm × 9–<u>14.9</u> (SD 2.6)–22 μm ($n = 85$).

Tetractines of canal walls: Equiangular and equiradiate, with conical, sharp-tipped actines, the basal system with slightly shorter actines than the smaller triactines (Fig. 11c). The apical actines are straight or slightly curved (Fig. 11b, inset). Tetractine dimensions of the actines of the basal system are (combined from 4 specimens, Table 6): 62–<u>121.4</u> (SD 17.0)–165 μm × 9–<u>12.3</u> (SD 1.5)–18 μm ($n = 80$). Dimensions of apical actines are (Porifera-KAUMM-9, measured in sections): 61–<u>86.7</u> (SD 24.4)–125 μm × 7–<u>8.3</u> (SD 1.0)–10 μm ($n = 5$).

Ecology: Specimens of this study occurred on reef walls and cave walls, under reef overhangs and in crevices, under coral rubble, always on hard substrate. Sometimes they were growing in illuminated parts of the reef. Specimens were collected from 0.5 m (reef flat, under coral rubble) to 20 m depth.

Distribution: *L. chagosensis* has a wide Indo-Pacific distribution (Red Sea, Indian Ocean, to Central Pacific, Wörheide and Hooper 1999). For the Red Sea, we here provide reports for *L. chagosensis* ranging from the Gulf of Aqaba (Dahab, Egypt) in the north to the middle/southern Red Sea near Al Lith, Saudi Arabia (Fig. 11d).

Remarks: *Leucetta chagosensis* was described from Chagos in the Indian Ocean (Dendy 1913). In contrast to *L. microraphis* from the Red Sea (as described below), the giant triactines are restricted to the cortical skeleton and the two species differ in their life colour so strikingly that they can easily be distinguished. In the original description of *L. chagosensis*, no tetractines are mentioned (Dendy 1913), but these are present in a spicule preparation of the holotype (own observations, see Table 6). In the holotype (BMNH 1920.12.9.51), small triactines are larger than in the Red Sea specimens, but the tetractines are of similar size (Table 6). Because only fragmented large triactines were present in the holotype spicule preparation, we cannot provide measurements here. Dendy (1913) mentioned sizes about 590 μm, which exceeds the sizes of large triactines of Red Sea *L. chagosensis* specimens (although the largest triactines are only slightly smaller, Table 6). Molecular studies have repeatedly shown that *Leucetta chagosensis* is likely a complex of cryptic species, which are genetically divergent. Some of the genetic lineages occur sympatrically for example at the Great Barrier Reef (Wörheide et al. 2002, 2008). *Leucetta chagosensis* from the Red Sea forms a distinct genetic clade, which is closely related to Maldivian specimens (Wörheide et al. 2008). However, how both of these are related to specimens from the type locality is unknown, and it is possible that the Maldivian specimens are genetically identical to the ones of Chagos. Therefore, the genetic clades of *L. chagosensis* await taxonomic revision, which may require—aside from detailed morphological inspections—the consideration of genetic diagnostic characters.

Leucetta microraphis Haeckel, 1872
(Figure 12a-d, Suppl. Fig. 9, Table 7)

Synonymised names: *Leucaltis floridana* var. *australiensis* Carter, 1886; *Leucandra carteri* Dendy, 1893; *Leucetta carteri* (Dendy, 1892); *Leucetta microrhaphis* Haeckel, 1872; *Leucetta primigenia* var. *microraphis* Haeckel, 1872.

Material examined: 7 specimens SNSB-BSPG GW3028, SNSB-BSPG GW3144, SNSB-BSPG GW3163, SNSB-BSPG GW3164, SNSB-BSPG GW3196, SMF11581, Porifera-KAUMM-12

Localities: SMF11581: Duba, Saudi Arabia N27.344361° E35.694861°, coll. D. Erpenbeck, 18 June 2013; SNSB-BSPG GW3144: Thuwal Reefs (Palace Reef North) N22.305447° E38.962214°, 10–25 m depth, coll. G. Wörheide, 28 April 2013; SNSB-BSPG GW3028 Thuwal Reefs (Shi'b Esfenj), Saudi Arabia: N22.216333° E38.948583°, 10–25 m depth, coll. G. Wörheide, 23 April 2013; SNSB-BSPG GW3196: Thuwal Reefs (Abu Madafi North) N22.086947° E38.781958°, 10–25 m depth, coll. G. Wörheide, 30 April 2013; SNSB-BSPG GW3163, SNSB-BSPG GW3164: Thuwal Reefs (Abu Madafi centre) N22.062093° E 38.763701°, 10–25 m depth, coll. G. Wörheide, 29 April 2013; Porifera-KAUMM-12: Saudi Arabia, NE of Al Lith, Saudi Arabia N20.19959°; E40.04422°, 8 m depth, coll. O. Voigt, 7 March 2012.

OTU (C-region): OTU 10, sequence identity 99.9% ($n = 7$).

Colour: pinkish or pinkish-white or light purple in life, beige to white in 80% ethanol

Growth form: Massive, globular, of about 1.8 to 4.7 cm with one or few large apical oscular openings with a diameter from 2.4 to 5.5 mm. Large tangential triactines sometimes visible by eye on the sponge surface (Fig. 12a, Suppl. Fig. 9).

Aquiferous system: Leuconoid.

Skeleton: Cortical skeleton with tangentially arranged giant triactines along with smaller sized triactines. The

Fig. 12 *Leucetta microraphis* (OTU 10). **a** Specimen SNSB-BSPG GW3163 *in situ*. **b** Section through sponge wall (SMF11581). **c** Spicules (SMF11581): Giant triactines (tria I), small triactines (tria II), and tetractines (tetr). Inset: apical actine of tetractine, protruding into the lumen of a canal. **d** Localities of collected specimens. cx = cortex. tetr = tetractine; tria = triactine
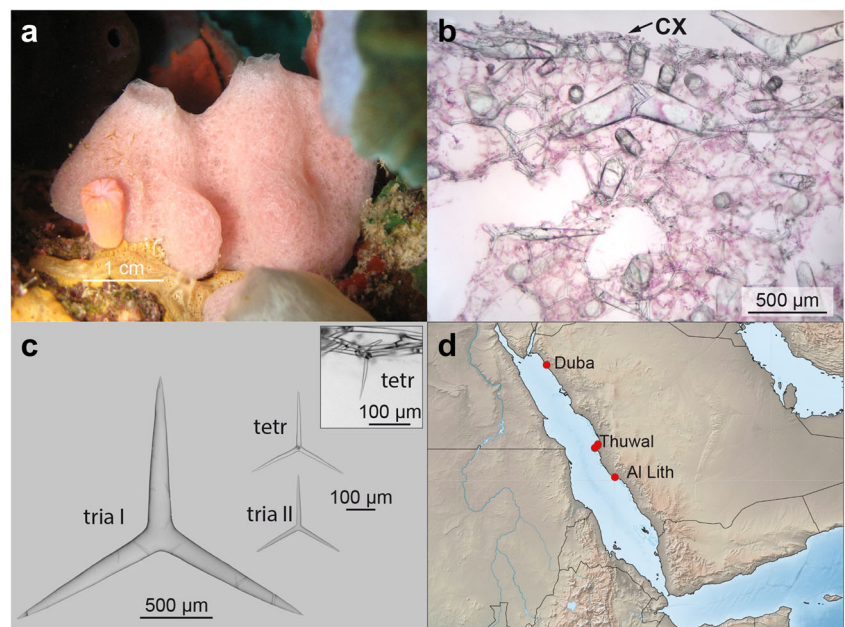
Table 7 Spicule sizes of *L. microraphis*

Spicule / Specimen	Actine length in µm				Actine width in µm				Mean length/width	n
	Min	Mean	SD	Max	Min	Mean	SD	Max		
Large cortical triactines										
SMF11581	447	1029.3	233.9	1488	89	149.9	28.2	210	6.8	20
Porifera-KAUMM-12	392	627.3	211.3	1069	41	74.4	23.1	123	8.4	20
combined	**392**	**828.3**	**297.9**	**1488**	**41**	**109.4**	**45.6**	**210**	**7.6**	**40**
L. microraphis Indonesia*	1175	1536.0	–	1980	132	169.3	–	216	9.1	25
L. microraphis Australia**	460	705.2	–	940	60	91.2	–	120	7.7	25
Triactines										
SMF11581	120	164.4	21.1	213	14	18.5	2.3	24	8.9	20
Porifera-KAUMM-12	123	169.7	22.5	211	12	16.4	2.0	20	10.4	20
combined	**120**	**167.0**	**21.9**	**213**	**12**	**17.5**	**2.4**	**24**	**9.6**	**40**
L. microraphis Indonesia*	99	175.7	–	270	8	15.8	–	33	11.1	25
L. microraphis Australia**	140	169.4	–	240	14	18.2	–	28	9.3	25
Tetractines (basal actines)										
SMF11581	110	165.2	20.2	220	13	16.7	2.1	21	9.9	20
Porifera-KAUMM-12	112	146.7	15.7	183	10	13.1	1.8	17	11.3	20
combined	**110**	**156.0**	**20.3**	**220**	**10**	**14.9**	**2.6**	**31**	**10.4**	**40**
L. microraphis Indonesia*	135	–	–	150	9	–	–	12	–	25
L. microraphis Australia**	110	143.4		165	12	14.4		20	10.0	25
Tetractines (apical actines)										
SMF11581	73	130.6	35.2	180	8	10.3	1.7	13	12.7	13
L. microraphis Indonesia*	50	–	–	70	–	–	–	–	–	

(*Min* minimum, *SD* standard deviation, *Max* maximum). Mean values are underlined; n gives the number of measured spicules. *Measurements from Van Soest and De Voogd (2015); ** Measurements from Wörheide and Hooper (1999)

choanosomal skeleton also contains scattered giant triactines and smaller triactines (Fig. 12b). Tetractines of similar size as the small triactines occur in the wall of presumably exhalant canals, their basal actines tangential to the canal wall, and the apical actine reaching inside the lumen of the canal (Fig. 12c, inset).

Spicules: *Triactines I*: Giant triactines of the cortical and the choanosomal skeleton, equiangular, and equiradiate, with conical, sharp-tipped actines (Fig. 12c). Triactine I dimensions are (combined from two specimens, Table 7): 392–828.3 (SD 297.9)–1488 µm × 41–109.4 (SD 45.6)–210 µm (*n* = 40).

Triactines II: Smaller triactines from the cortical and choanosomal skeleton, equiangular and equiradiate, with conical, sharp-tipped actines. Triactine II dimensions are (combined from two specimens, Table 7): 120–167.0 (SD 21.9)–213 µm × 12–17.5 (SD 2.4)–24 µm (*n* = 40).

Tetractines of the canal walls: Equiradiate and equiangular, with conical, sharp-tipped actines. Dimensions of the basal actines are: 110–156.0 (SD 20.3)–220 µm × 10–14.9 (SD 2.6)–31 µm (*n* = 40); apical actines (measured in sections of specimen SMF11581): 73–130.6 – (SD 35.2)–180 µm × 8–10.3 (SD 1.7)–13 µm (*n* = 13) (Fig. 12c, inset).

Ecology: Growing on hard substrate, under reef overhangs, in crevices, or on the underside of larger pieces of coral rubble. Sampled from 8 m to ca. 25 m depth.

Distribution: We report finding this species from the northern Red Sea (Duba) to the middle/southern Red Sea (Al Lith). The species also occurs in Indonesia, Papua New Guinea, New Caledonia and tropical Australia.

Remarks: As pointed out by Van Soest and De Voogd (2015), the species requires a thorough revision. Haeckel (1872) described *L. microraphis* as a variety of *Leucetta primigenia* Haeckel, 1872. The diagnosis of *L. primigenia* is very unspecific, describing all triactines to be of "very variable size". The three varieties of the species differ in the abundance of different size categories of triactines: *L. primigenia* var. *isoraphis* lacks giant triactines, in *L. primigenia* var. *microraphis* small triactines were more frequent than giant triactines, and in *L. primigenia* var. *megaraphis* the majority of triactines is of giant size. Compared to our specimens, *L. microraphis* from Indonesia (Van Soest and De Voogd 2015) had larger giant triactines (mean 1,536 µm × 169.3), and while the ratio actine length to actine width also differed in comparison to the Red Sea specimens, it is also variable in the latter (Table 7). An Australian specimen (Wörheide and

Hooper 1999) was more similar to the Red Sea specimens regarding spicule sizes (Table 7), but was brown in life. Alive specimens from Indonesia and the Red Sea show nuances of pink. It remains to be tested whether these differences in spicule sizes and body colour reflect geographic variation or not.

Discussion

Diversity of Red Sea Calcinea

We document 10 calcinean species in the Red Sea, of which four are new, one (*B. aff. aspina*) is new to the Red Sea, one ("*Clathrina*" aff. *adusta*, OTU3) remains morphologically undetermined, and four were previously documented from the Red Sea (*Clathrina sinusarabica*, *Arthuria sueziana*, *Leucetta chagosensis*, *Leucetta microraphis*). In our survey we were not able to find the following species that were previously reported from the Red Sea (Haeckel 1872; Row 1909): *Arthuria darwini*, *Clathrina primordialis*, and *Leucetta primigenia*. *Clathrina primordialis* and *Leucetta primigenia*, both *sensu* Haeckel 1872, probably included multiple species, as is reflected by their supposed morphological variability and their cosmopolitan distribution. Biochemical and DNA-data have shown that such cosmopolitan species comprise morphologically similar, but distinct species (Klautau et al. 1994, 2013). *Clathrina primordialis* is now considered to be restricted to the Mediterranean (Klautau and Valentine 2003), the type locality is in the Adriatic (Klautau et al. 2016). Therefore, it remains unclear, what species "*C. primordialis*" from the Red Sea might represent, but potentially Haeckel (1872) and Row (1909) referred to specimens that were conspecific with *C. rowi* sp. nov. The ITS sequence of *C. primordialis* from the Mediterranean was not closely related to any sampled *Clathrina* species from the Red Sea (Suppl. Fig. 1).

The description of *Leucetta primigenia* is similarly very unspecific, and included *Leucetta microraphis* as a variant (see Results: OTU 10, remarks). Row (1909) mentions *Leucetta primigenia* (1 specimen) and "*Leucetta primigenia* var. *microraphis*" (two specimens) from the Red Sea. Possibly, *L. primigenia* from the Red Sea is identical with *Leucetta chagosensis* or another *Leucetta* species that was not sampled by us.

The Red Sea Calcinea of our collection represent a broad taxonomic range of the subclass: according to our phylogeny the species are not restricted to only few clades, but are distributed all over the tree (Fig. 2). In addition to provide new species, our material also extended the sample size and known distribution of known species in the Red Sea. *Ernstia arabica* sp. nov. shows the widest range, occurring from Gulf of Aqaba in the north to the Farasan Islands in the south, but could not be found in several of the intermediate sites (Fig. 4e). *Leucetta chagosensis*

and *L. microraphis* were also sampled at multiple locations, from the northern Red Sea (Dahab, for *L. chagosensis*, Duba for *L. microraphis*) to Al Lith in the south. *Clathrina sinusarabica* and *C. rowi* sp. nov. are so far missing from the north and the south of the Red Sea. However, additional sampling efforts will likely extend the known range of all these species.

Phylogeny

The LSU phylogeny shows many similarities to previous results (e.g. Voigt and Wörheide 2016). A problem that remains to be solved is the low support for the position of the root within Calcinea, which neither was resolved with larger datasets (including almost the complete LSU and the small subunit RNA gene or 18S, Voigt et al. 2012a). This will require the application of additional DNA markers to LSU and ITS, because the latter is too variable to include Calcaronea as outgroup (Klautau et al. 2013). Solving this rooting problem is also crucial to evaluate the monophyly of *Ascandra* and *Soleneiscus* and the relationship of *Levinella*, which in our tree (Fig. 2) is impacted by the position of the root that differed from previous results of a larger ribosomal RNA gene dataset (Voigt et al. 2012a). The short C-region however could recover clades of *Ernstia*, *Clathrina sensu* Klautau 2013, *Brattegardia*, *Borojevia*, *Leucettusa*, and *Leucettidae*. According to our phylogeny, the status of "*Clathrina*" *adusta* also has to be reconsidered. More recently it was allocated to *Ernstia* (Klautau et al. 2013), but subsequent DNA analyses showed that "*C*". *adusta* is not closely related to the type species of *Ernstia* (Voigt and Wörheide 2016). In the latter work, "*C*". *adusta* was suggested to belong to the genus *Arthuria*, because this was the only other genus to which it could be diagnosed due to the tetractines that occur in its skeleton (Voigt and Wörheide 2016). However, no LSU sequence of other *Arthuria* species was available to verify this taxonomic placement. As our phylogeny now contains *Arthuria sueziana*, we can now clearly state that "*C*". *adusta* also is not a member of *Arthuria*. Instead, "*C*". *adusta* and other undetermined calcinean specimens (including OTU3) form the sister clade to *Clathrina* sensu Klautau et al. (2013), but differ morphologically by containing tetractines. Possibly it will be necessary to establish a new genus for "*C*". *adusta* and related tetractine-bearing species that cannot be attributed to known genera.

The LSU C-region as barcoding marker of Calcinea

The mitochondrial cytochrome oxidase subunit I gene (COI) was suggested as standard barcoding marker for many animal groups (Hebert et al. 2003), including demosponges (Wörheide et al. 2007). However, calcareous sponge mitochondrial genomes have several peculiarities, like a modified genetic code (Lavrov et al. 2013) and extraordinary mutation rates (Voigt et al. 2012b; Lavrov et al. 2013, 2016), which

makes the application of standard mitochondrial primers for DNA barcoding impossible. Therefore, the C-region of LSU was suggested as a possible alternative (Voigt and Wörheide 2016).

With the Red Sea collection of Calcinea, we now could demonstrate that the C-region of LSU is indeed a useful marker for DNA barcoding approaches to study the diversity for a whole geographical region. All our OTUs with more than one specimen show sequence identities of 99.5% and above. It remains uncertain if the marker provides a true barcoding gap (Meyer and Paulay 2005) between all calcinean species, i.e. if the interspecific variation is larger than intraspecific variation. Currently, for most other species only one sequence is available, and from our OTUs, only *C. sinusarabica* and *C. rowi* were relatively closely related (Fig. 2). In this case, 14 synapomorphic substitutions occur between the species, and intraspecific variation is much smaller than interspecific variation (see Suppl. Fig. 5). However, despite the fact that our sampling to date is the most comprehensive largest collection of the Red Sea Calcinea, the sample numbers per species are still low (max. 11), and the addition of more species and specimens from other regions may show that a barcoding gap between two closely related species is not always present. For example, the two morphospecies *Clathrina helveola* and *Clathrina wistariensis* from Australia (Fig. 2) have identical barcode sequences (Voigt and Wörheide 2016). Alternatively, it is also possible, that the morphological differences between these two species (e.g. the life body colour, Wörheide and Hooper 1999) in fact represent intraspecific variation. Additional DNA markers may supplement the C-region of LSU as DNA barcoding marker in such problematic cases.

DNA barcode approaches will be very helpful in order to detect intraspecific morphological variation in calcareous sponges. For example, the taxonomic value of presence or absence of trichoxea as a diagnostic character has been discussed in the distinction between *Arthuria (Clathrina) canariensis* and *Arthuria (Clathrina) tenuipilosa*: While, e.g., Thacker (1908) considered presence or absence of trichoxea as not important and that the species should be considered identical, other authors did not follow his opinion and considered such differences as important enough to separated the species (Row 1909; Klautau and Valentine 2003). In contrast, with *C. rowi* sp. nov., we interpreted the occurrence of many trichoxea-like diactines in one specimen (SMF11633) as intraspecific variation (see Results, *C. rowi* sp. nov.), a decision supported by our DNA barcoding results and the morphological similarity of triactines of this OTUs specimens. If our interpretation is correct, it can be expected to find intermediate specimens with less frequent trichoxeas. As this example shows, DNA barcoding can provide new testable hypotheses about species identity under different species concepts. Despite our findings for *C. rowi* sp. nov., the presence/absence of trichoxeas may have taxonomic value in other species. In fact, the difficulties to distinguish intraspecific from interspecific morphological variation may have caused

many of the problems we observe in the systematics of calcareous sponges. In this regard, DNA-supported studies and integrative systematics have helped in recent times to approach towards phylogenetically meaningful systematics of Calcarea, especially in the suborder Calcinea (Rossi et al. 2011; Klautau et al. 2013). DNA analyses should become a standard technique especially in the description of new species, complementing thorough morphological observations. The full diversity of Calcarea is not very well known, as our work and other recent integrative works show (e.g., Imešek et al. 2014; Azevedo et al. 2015), and new species are frequently discovered. DNA barcoding approaches can accelerate the discovery of new species, by binning specimens into DNA-based OTUs, which are then compared to DNA databases of morphologically characterized specimens. Prerequisite for DNA barcoding approaches remains the formation of comprehensive reference databases as the Sponge Barcoding Database (www.spongebarcoding.org, Wörheide et al. 2007). At its current stage, the Sponge Barcoding Database does still not include enough reference sequences of morphologically inspected calcinean specimens. With the data provided here, we offer a first comprehensive barcoding collection of calcinean sponges for the Red Sea ecoregion. It can serve as starting point for DNA-based diversity surveys, including the identification of incomplete or morphologically poorly preserved specimens.

References

Abràmoff MD, Magalhães PJ, Ram SJ (2004) Image processing with image. J Biophotonics Int 11:36–42

Adlard RD, Lester RJG (1995) Development of a diagnostic test for *Mikrocytos roughleyi*, the aetiological agent of Australian winter mortality of the commercial rock oyster, *Saccostrea commercialis* (Iredale & Roughley). J Fish Dis 18:609–614

Allen JE, Whelan S (2014) Assessing the state of substitution models describing noncoding RNA evolution. Genome Biol Evol 6:65–75

Azevedo F, Hajdu E, Willenz P, Klautau M (2009) New records of calcareous sponges (Porifera, Calcarea) from the Chilean coast. Zootaxa 2072:1–30

Azevedo F, Cóndor-Luján B, Willenz P et al (2015) Integrative taxonomy of calcareous sponges (subclass Calcinea) from the Peruvian coast: morphology, molecules, and biogeography. Zool J Linnean Soc 173: 787–817

Borojević R, Boury-Esnault N, Vacelet J (1990) A revision of the supraspecific classification of the subclass Calcinea (Porifera, class Calcarea) Bulletin du Museum National d'Histoire Naturelle Section A. Zoologie Biologie et Ecologie Animales 12:243–276

Borojević R, Boury-Esnault N, Manuel M, Vacelet J (2002) Clathrinida. In: Systema Porifera: A Guide to the Classification of Sponges. pp 1141–1152

Castresana J (2000) Selection of conserved blocks from multiple alignments for their use in phylogenetic analysis. Mol Biol Evol 17:540–552

Chombard C, Boury-Esnault N, Tillier S (1998) Reassessment of homology of morphological characters in tetractinellid sponges based on molecular data. Syst Biol 47:351–366

Dendy A (1891) A monograph of the Victorian sponges, I. The organisation and classification of the Calcarea Homocoela, with descriptions of the Victorian species. Trans Royal Soc Vic 3:1–81

Dendy A (1905) Report on the sponges collected by Professor Herdman, at Ceylon in 1902. In: Herdman WA (ed) Report to the government of Ceylon on the pearl oyster fisheries of the Gulf of Manaar. Royal Society, London, pp 57–246

Dendy A (1913) Report on the calcareous sponges collected by H.M.S. Sealark" in the Indian Ocean. Trans Linnean Soc London, Zool 16:1–29

DiBattista J, Roberts MB, Bouwmeester J et al (2016) A review of contemporary patterns of endemism for shallow water reef fauna in the Red Sea. J Biogeogr 43:423–439

Dohrmann M, Voigt O, Erpenbeck D, Wörheide G (2006) Non-monophyly of most supraspecific taxa of calcareous sponges (Porifera, Calcarea) revealed by increased taxon sampling and partitioned Bayesian analysis of ribosomal DNA. Mol Phylogenet Evol 40:830–843

Erpenbeck D, Voigt O, Gültas M, Wörheide G (2008) The Sponge Genetree Server—providing a phylogenetic backbone for poriferan evolutionary studies. Zootaxa 1939:58–60

Erpenbeck D, Voigt O, Al-Aidaroos AM et al (2016) Molecular biodiversity of Red Sea demosponges. Mar Pollut Bull 105:507–514

Gouy M, Guindon S, Gascuel O (2010) SeaView version 4: a multiplatform graphical user interface for sequence alignment and phylogenetic tree building. Mol Biol Evol 27:221–224

Guindon S, Dufayard J-F, Lefort V et al (2010) New algorithms and methods to estimate maximum-likelihood phylogenies: assessing the performance of PhyML 3.0. Syst Biol 59:307–321

Haeckel E (1872) Die Kalkschwämme. Eine Monographie in zwei Bänden Text und einem Atlas mit 60 Tafeln Abbildungen. Verlag von Georg Reimer, Berlin

Hebert PDN, Cywinska A, Ball SL, deWaard JR (2003) Biological identifications through DNA barcodes. Proc Biol Sci 270:313–321

Imešek M, Pleše B, Pfannkuchen M et al (2014) Integrative taxonomy of four Clathrina species of the Adriatic Sea, with the first formal description of Clathrina rubra Sarà, 1958. Org Divers Evol 14:21–29

Jenkin CF (1908) The marine fauna of Zanzibar and British east Africa, from collections made by Cyril crossland, M.A., in the years 1901 & 1902.—The calcareous sponges. Proc Zool Soc London 78:434–456

Kearse M, Moir R, Wilson A et al (2012) Geneious basic: an integrated and extendable desktop software platform for the organization and analysis of sequence data. Bioinformatics 28:1647–1649

Keller C (1889) Die Spongienfauna des Rothen Meeres (I. Hälfte). Z Wiss Zool 48:311–405

Keller C (1891) Die Spongienfauna des Rothen Meeres (II. Hälfte). Z Wiss Zool 52:294–368

Klautau M, Borojevic R (2001) Sponges of the genus Clathrina Gray, 1867 from Arraial do Cabo, Brazil. Zoosystema 23:395–410

Klautau M, Valentine C (2003) Revision of the genus Clathrina (Porifera, Calcarea). Zool J Linnean Soc 139:1–62

Klautau M, Solé-Cava AM, Borojević R (1994) Biochemical systematics of sibling sympatric species of Clathrina (Porifera: Calcarea). Biochem Syst Ecol 22:367–375

Klautau M, Azevedo F, Cóndor-Luján B et al (2013) A molecular phylogeny for the order Clathrinida rekindles and refines Haeckel's taxonomic proposal for calcareous sponges. Integr Comp Biol 53:447–461

Klautau M, Imešek M, Azevedo F et al (2016) Adriatic calcarean sponges (Porifera, Calcarea), with the description of six new species and a richness analysis. Eur J Taxon 178:1–52

Lavrov DV, Pett W, Voigt O et al (2013) Mitochondrial DNA of Clathrina clathrus (Calcarea, Calcinea): six linear chromosomes, fragmented rRNAs, tRNA editing, and a novel genetic code. Mol Biol Evol 30: 865–880

Lavrov DV, Adamski M, Chevaldonné P, Adamska M (2016) Extensive mitochondrial mRNA editing and unusual mitochondrial genome organization in calcaronean sponges. Curr Biol 26:86–92

Manuel M, Borchiellini C, Alivon E et al (2003) Phylogeny and evolution of calcareous sponges: monophyly of Calcinea and Calcaronea, high level of morphological homoplasy, and the primitive nature of axial symmetry. Syst Biol 52:311–333

Meyer CP, Paulay G (2005) DNA barcoding: error rates based on comprehensive sampling. PLoS Biol 3:2229–2238

Minchin EA (1908) Materials for a monograph of the ascons. II: − The formation of spicules in the genus Leucosolenia, with some notes on the histology of the sponges. Q J Microsc Sci 52:301–355

Posada D (2008) jModelTest: phylogenetic model averaging. Mol Biol Evol 25:1253–1256

Ronquist F, Huelsenbeck JP (2003) MrBayes 3: Bayesian phylogenetic inference under mixed models. Bioinformatics 19:1572–1574

Rossi AL, de Moraes Russo CA, Solé-Cava AM et al (2011) Phylogenetic signal in the evolution of body colour and spicule skeleton in calcareous sponges. Zool J Linnean Soc 163:1026–1034

Row R (1909) Reports on the Marine Biology of the Sudanese Red Sea. XIII. Report on the sponges, collected by Mr. Cyril Crossland, 1904–5.–Part I. Calcarea. The Journal of the Linnean Society Zoology 31:182–214, pls. 19–20

Shorthouse DP (2010) SimpleMappr, an online tool to produce publication-quality point maps. In: SimpleMappr. http://www.simplemappr.net. Accessed 22 Jun 2016

Telford MJ, Wise MJ, Gowri-Shankar V (2005) Consideration of RNA secondary structure significantly improves likelihood-based estimates of phylogeny: examples from the Bilateria. Mol Biol Evol 22:1129–1136

Thacker AG (1908) On collections of the Cape Verde Islands fauna made by Cyril Crossland, M.A. The calcareous sponges. Proc Zool Soc London 49:757–782

Van Soest RWM, De Voogd N (2015) Calcareous sponges of Indonesia. Zootaxa 3951:1–105

Van Soest RWM, Boury-Esnault N, Hooper JNA, et al. (2016) World Porifera Database. In: World Porifera Database. http://www.marinespecies.org/porifera/. Accessed 10 Feb 2017

Vargas S, Schuster A, Sacher K et al (2012) Barcoding sponges: an overview based on comprehensive sampling. PLoS One 7, e39345

Villesen P (2007) FaBox: an online toolbox for fasta sequences. Mol Ecol Notes 7:965–968

Voigt O, Wörheide G (2016) A short LSU rRNA fragment as a standard marker for integrative taxonomy in calcareous sponges (Porifera: Calcarea). Org Divers Evol 16:53–64

Voigt O, Wülfing E, Wörheide G (2012a) Molecular phylogenetic evaluation of classification and scenarios of character evolution in calcareous sponges (Porifera, Class Calcarea). PLoS One 7, e33417

Voigt O, Eichmann V, Wörheide G (2012b) First evaluation of mitochondrial DNA as a marker for phylogeographic studies of Calcarea: a case study from *Leucetta chagosensis*. Hydrobiologia 687:101–106

Wörheide G, Hooper JNA (1999) Calcarea from the Great Barrier Reef. 1: Cryptic Calcinea from Heron Island and Wistari Reef (Capricorn-Bunker Group). Queensland Mus Mem 43:859–891

Wörheide G, Hooper JNA, Degnan BM (2002) Phylogeography of western Pacific *Leucetta* "*chagosensis*" (Porifera: Calcarea) from ribosomal DNA sequences: implications for population history and conservation of the Great Barrier Reef World Heritage Area (Australia). Mol Ecol 11:1753–1768

Wörheide G, Nichols SA, Goldberg J (2004) Intragenomic variation of the rDNA internal transcribed spacers in sponges (Phylum Porifera): Implications for phylogenetic studies. Mol Phylogenet Evol 33:816–830

Wörheide G, Erpenbeck D, Menke C (2007) The sponge barcoding project: aiding in the identification and description of poriferan taxa. In: Custódio MR, Lôbo-Hajdu G, Hajdu E, Muricy G (eds) Porifera research: biodiversity, innovation and sustainability. Museu Nacional, Rio de Janeiro, pp 123–128

Wörheide G, Epp L, Macis L (2008) Deep genetic divergences among Indo-Pacific populations of the coral reef sponge *Leucetta chagosensis* (Leucettidae): founder effects, vicariance, or both? BMC Evol Biol 8:24